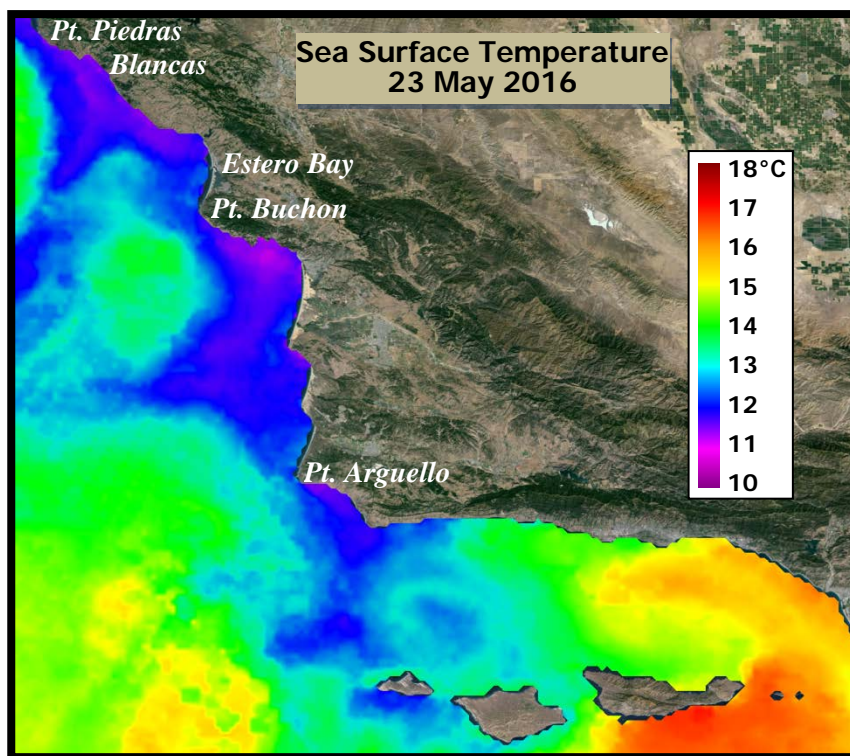


**City of Morro Bay and  
Cayucos Sanitary District**

# **OFFSHORE MONITORING AND REPORTING PROGRAM**

## **SECOND QUARTER RECEIVING-WATER SURVEY**

**MAY 2016**



**Marine Research Specialists**  
3140 Telegraph Rd., Suite A  
Ventura, California 93003

**Report to the  
City of Morro Bay and  
Cayucos Sanitary District**

**955 Shasta Avenue  
Morro Bay, California 93442  
(805) 772-6272**

**OFFSHORE MONITORING  
AND REPORTING PROGRAM**

**SECOND QUARTER  
RECEIVING–WATER SURVEY**

**MAY 2016**

**Prepared by  
Douglas A. Coats**

**Marine Research Specialists**

**3140 Telegraph Rd., Suite A  
Ventura, California 93003**

**Telephone: (805) 644-1180**

**Telefax: (805) 289-3935**

**E-mail: [Marine@Rain.org](mailto:Marine@Rain.org)**

**June 2016**

# marine research specialists

3140 Telegraph Road, Suite A • Ventura, CA 93003 • (805) 644-1180

Bruce Keogh  
Wastewater Division Manager  
City of Morro Bay  
955 Shasta Avenue  
Morro Bay, CA 93442

14 June 2016

**Reference: Second Quarter Receiving-Water Survey Report – May 2016**

Dear Mr. Keogh:

The attached report presents results from a quarterly receiving-water survey conducted on Tuesday, 24 May 2016. The survey was conducted in accordance with the requirements of the NPDES permit issued to the City and District for discharge of treated wastewater to Estero Bay. The report evaluated compliance with permit limitations and assessed the effectiveness of effluent dispersion. Quantitative analyses of continuous instrumental measurements and qualitative visual observations confirm that the wastewater discharge complied with the receiving-water limitations specified in the permit, and with the objectives of the California Ocean Plan.

The offshore measurements confirmed that the diffuser structure and treatment plant continued to operate at a high level of performance. The measurements delineated a diffuse discharge plume containing low organic loads within a highly localized region southwest of the discharge point. Dilution within the plume exceeded expectations based on modeling and outfall design criteria.

Please contact the undersigned if you have questions regarding the attached report.

Sincerely,



Douglas A. Coats  
Program Manager

I certify under penalty of law that this document and all attachments were prepared under my direction or supervision in accordance with a system designed to assure that qualified personnel properly gather and evaluate the information submitted. Based on my inquiry of the person or persons who manage the system, or those persons directly responsible for gathering the information, the information submitted is, to the best of my knowledge and belief, true, accurate, and complete. I am aware that there are significant penalties for submitting false information, including the possibility of fine and imprisonment for knowing violations.

  
\_\_\_\_\_  
Mr. Bruce Keogh  
Wastewater Division Manager  
City of Morro Bay

Date June 15, 2016

## TABLE OF CONTENTS

LIST OF FIGURES .....	i
LIST OF TABLES .....	ii
INTRODUCTION .....	1
SURVEY SETTING .....	1
SAMPLING LOCATIONS .....	3
OCEANOGRAPHIC PROCESSES .....	7
METHODS .....	9
<i>Auxiliary Measurements</i> .....	10
<i>Instrumental Measurements</i> .....	10
<i>Quality Control</i> .....	12
RESULTS.....	12
<i>Auxiliary Observations</i> .....	12
<i>Instrumental Observations</i> .....	14
<i>Outfall Performance</i> .....	22
COMPLIANCE.....	25
<i>Permit Provisions</i> .....	26
<i>Screening of Measurements</i> .....	26
<i>Other Lines of Evidence</i> .....	30
CONCLUSIONS.....	32
REFERENCES .....	32

## LIST OF FIGURES

<b>Figure 1.</b> Location of the Receiving-Water Survey Area.....	2
<b>Figure 2.</b> Station Locations.....	4
<b>Figure 3.</b> Drogued Drifter Trajectory .....	7
<b>Figure 4.</b> Tidal Level during the May 2016 Survey .....	8
<b>Figure 5.</b> Schematic of Upwelling Processes .....	8
<b>Figure 6.</b> Five-Day Average Upwelling Index ( $\text{m}^3/\text{s}/100$ m of coastline) .....	9
<b>Figure 7.</b> CTD Tracklines during the May 2016 Tow Surveys.....	11
<b>Figure 8.</b> Vertical Profiles of Water-Quality Parameters .....	18
<b>Figure 9.</b> Horizontal Distribution of Mid-Depth Water-Quality Parameters 9.01 m below the Sea Surface.....	20
<b>Figure 10.</b> Horizontal Distribution of Shallow Water-Quality Parameters 3.48 m below the Sea Surface .....	21
<b>Figure 11.</b> Mid-Depth Plume Dilution Computed from Salinity Anomalies in Figure 9b.....	24
<b>Figure 12.</b> Shallow Plume Dilution Computed from Salinity Anomalies in Figure 10b.....	25

**LIST OF TABLES**

**Table 1.** Target Locations of the Receiving-Water Monitoring Stations ..... 4

**Table 2.** Average Position of Vertical Profiles during the May 2016 Survey ..... 6

**Table 3.** CTD Specifications..... 10

**Table 4.** Standard Meteorological and Oceanographic Observations..... 13

**Table 5.** Vertical Profile Data Collected on 24 May 2016 ..... 15

**Table 6.** Permit Provisions Addressed by the Offshore Receiving-Water Surveys..... 25

**Table 7.** Receiving-Water Measurements Screened for Compliance Evaluation..... 27

**Table 8.** Compliance Thresholds ..... 29

## **INTRODUCTION**

The City of Morro Bay and the Cayucos Sanitary District (MBCSD) jointly own the wastewater treatment plant operated by the City of Morro Bay. In March 1985, Region IX of the U.S. Environmental Protection Agency (USEPA) and the Central Coast California Regional Water Quality Control Board (RWQCB) issued the first National Pollutant Discharge Elimination System (NPDES) permit to the MBCSD. The permit incorporated partially modified secondary treatment requirements for the plant's ocean discharge. The permit has been re-issued three times, in March 1993 (RWQCB-USEPA 1993ab), December 1998 (RWQCB-USEPA 1998ab), and January 2009 (RWQCB-USEPA 2009). The May 2016 field survey described in this report was the thirtieth receiving-water survey conducted under the current permit.

The NPDES discharge permit requires seasonal monitoring of offshore receiving-water quality with quarterly surveys. This report summarizes the results of sampling conducted on 24 May 2016. Specifically, this second-quarter survey captured ambient oceanographic conditions along the central California coast during the spring season. The survey's measurements were used to assess the discharge's compliance with the objectives of the California Ocean Plan (COP) and the Central Coast Basin Plan (RWQCB 1994) as promulgated by the receiving-water limitations specified in the NPDES discharge permit.

The monitoring objectives were achieved by empirically evaluating tabulations of instrumental measurements and standard field observations. In addition to the traditional, vertical water-column profiles, instrumental measurements were used to generate horizontal maps from high-resolution data gathered by towing a CTD<sup>1</sup> instrument package repeatedly over the diffuser structure. This allowed for a more precise delineation of the plume's lateral extent.

## **SURVEY SETTING**

The MBCSD treatment plant is located within the City of Morro Bay, which is situated along the central coast of California halfway between Los Angeles and San Francisco. Effluent is carried from the onshore treatment plant through a 1,450-m long outfall pipe, which terminates at a diffuser structure on the seafloor 827 m from the shoreline within Estero Bay (Figure 1). The diffuser structure extends an additional 52 m toward the northwest from the outfall terminus and consists of 34 ports that are hydraulically designed to create a turbulent ejection jet that rapidly mixes effluent with receiving seawater upon discharge. Currently, six of the diffuser ports are kept closed, thereby improving effluent dispersion by increasing the ejection velocity from the remaining 28 ports distributed along a 42-m section of the diffuser structure.

Following discharge from the diffuser ports, additional turbulent mixing occurs as the buoyant plume of dilute effluent ascends through the water column. Most of this buoyancy-induced mixing occurs within a zone of initial dilution (ZID), whose lateral reach in modeling studies extends 15.2 m from the centerline of the diffuser structure. Beyond the ZID, energetic waves, tides, and coastal currents within Estero Bay further disperse the dilute effluent within the open-ocean receiving waters. Both vertical hydrocasts and horizontal tow surveys are conducted around the diffuser structure to assess the efficacy of the diffuser, to define the lateral extent of the discharge plume, and to evaluate compliance with the NPDES permit limitations.

---

<sup>1</sup> Conductivity, temperature, and depth (CTD)



**Figure 1.** Location of the Receiving-Water Survey Area

Near the diffuser, prevailing flow generally follows bathymetric contours that parallel the north-south trend of the adjacent coastline. Because of the rapid initial mixing achieved within 15 m of the diffuser structure, impingement of unmixed effluent onto the adjacent coastline, 827 m away, is highly unlikely. Nevertheless, in the event of a failure in the treatment plant's disinfection system, collection and analysis of water samples at the eight surfzone-sampling stations shown in Figure 1 would be conducted to monitor for potential shoreline impacts. These surfzone samples would be analyzed for total and fecal coliform, and enterococcus bacterial densities.

Areas of special concern, such as the Morro Bay National Estuary and the Monterey Bay National Marine Sanctuary, are not affected by the discharge because they are even more distant from the outfall location. For example, the southern boundary of the Monterey Bay National Marine Sanctuary is located 38 km to the north, while the entrance to the Morro Bay National Estuary lies 2.8 km south. The southerly orientation of the mouth of the Bay, and the presence of Morro Rock 2 km to the south, serve to further limit direct seawater exchange between the discharge point and the Bay (Figure 1).

### **SAMPLING LOCATIONS**

As shown in Figure 2, the offshore sampling pattern consists of six fixed offshore stations located within 100 m of the outfall diffuser structure. The red ⊕ symbols in the Figure indicate the target locations of the sampling stations (Table 1). The stations are situated at three distances relative to the center of the diffuser structure, and lie along a north-south axis at the same water depth (15.2 m) as the center of the diffuser. Depending on the direction of the local oceanic currents at the time of sampling, the discharge may influence one or more of these stations. The up-current stations on the opposite side of the diffuser then act as reference stations. Comparisons between the water properties at these antipodal stations quantify departures from ambient seawater properties caused by the discharge and allow compliance with the NPDES discharge permit to be determined.

The finite size of the diffuser is an important consideration in the assessment of wastewater dispersion close to the discharge. Although the discharge is considered a "*point source*" for modeling and regulatory purposes, it does not occur at a single isolated point of infinitesimal size. Instead, the discharge is distributed along a 42 m section of the seafloor, and, ultimately, the amount of wastewater dispersion at a given point in the water column is dictated by its distance from the closest diffuser port, rather than its distance from the center of the diffuser structure. This "*closest approach*" distance can be considerably less than the centerpoint distance normally cited in modeling studies (last two columns of Table 1).

Another important consideration for compliance evaluation is the ability to determine the actual location of the measurements. Discerning small spatial separations within the compact sampling pattern only became feasible after the advent of Differential Global Positioning Systems (DGPS). The accuracy of traditional navigation systems such as LORAN or standard GPS is typically  $\pm 15$  m, a span equal to half the total width of the ZID itself. DGPS incorporates a second signal from a fixed, land-based beacon that continuously transmits position errors in standard GPS readings to the DGPS receiver onboard the survey vessel. Real-time correction for these position errors provides an extremely stable and accurate offshore navigational reading with position errors of no more than 2 m, and often of sub-meter accuracy.

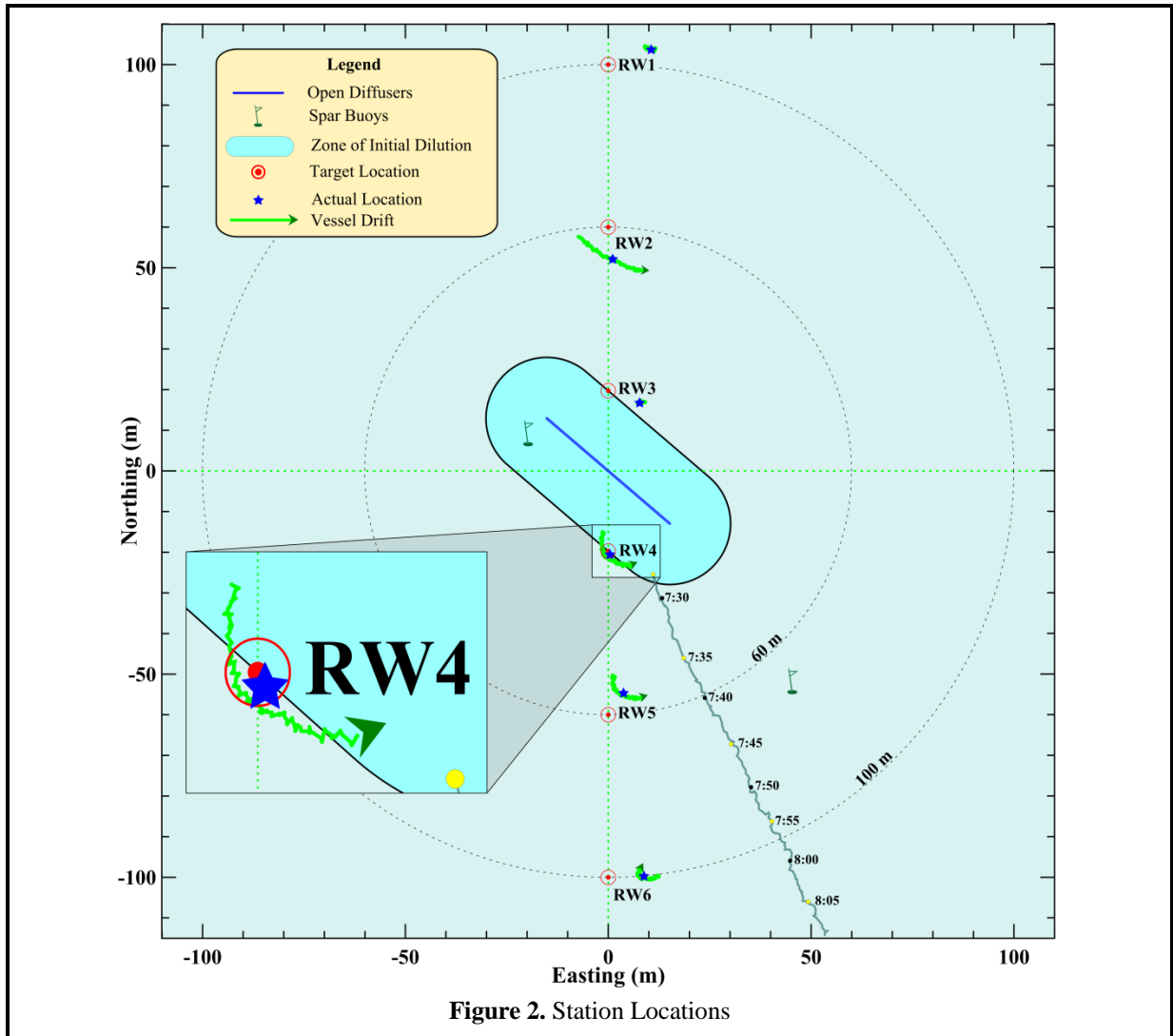


Figure 2. Station Locations

Table 1. Target Locations of the Receiving-Water Monitoring Stations

Station	Description	Latitude	Longitude	Center Distance <sup>2</sup> (m)	Closest Approach Distance <sup>3</sup> (m)
RW1	Upcoast Midfield	35° 23.253' N	120° 52.504' W	100	88.4
RW2	Upcoast Nearfield	35° 23.231' N	120° 52.504' W	60	49.4
RW3	Upcoast ZID	35° 23.210' N	120° 52.504' W	20	15.0
RW4	Downcoast ZID	35° 23.188' N	120° 52.504' W	20	15.0
RW5	Downcoast Nearfield	35° 23.167' N	120° 52.504' W	60	49.4
RW6	Downcoast Midfield	35° 23.145' N	120° 52.504' W	100	88.4

<sup>2</sup> Distance to the center of the open diffuser section

<sup>3</sup> Distance to the closest open diffuser port

During a diver survey in July 1998, the survey vessel's DGPS navigation system, consisting of a Furuno™ GPS 30 and FBX2 differential beacon receiver, was used to precisely determine the position of the open section of the diffuser structure (MRS 1998) and establish the target locations for the receiving-water monitoring stations shown in Figure 2 and listed in Table 1. Presently, the use of two independent DGPS receivers onboard the survey vessel allows access to two separate land-based beacons for navigational intercomparison, ensuring extremely accurate and uninterrupted navigational reports.

Recording of DGPS positions at one-second intervals allows precise determination of sampling locations throughout the vertical CTD profiling conducted at the six individual stations, as well as during the tow survey. Knowledge of the precise location of individual CTD measurements relative to the diffuser is critical for accurate interpretation of the water-property fields. During vertical-profile sampling, the actual measurement locations rarely coincide with the target coordinates listed in Table 1 because winds, waves, and currents induce unavoidable horizontal offsets (drift). Even during quiescent metocean<sup>4</sup> conditions, the residual momentum of the survey vessel as it approaches the target locations can create perceptible offsets. Using DGPS however, these offsets can be quantified, and the vessel location can be precisely tracked throughout sampling at each station.

The downcasts during the May 2016 survey were conducted progressing from north to south, beginning with Station RW1. The magnitude of the drift at each of the six stations during the May 2016 survey is apparent from the length of the green tracklines in Figure 2. The tracklines trace the horizontal movement of the CTD as it was lowered to the seafloor at each station. Their lengths and offsets from the target locations reflect the overall station-keeping ability during the May 2016 survey.

The time it took the CTD to traverse the water column to the seafloor, which averaged 1 min 12 s, was consistent among stations, while the lateral distance traversed by the instrument package varied considerably among the stations (Figure 2). The lateral movement of the CTD movement at any given time is typically determined by a complex interplay between the external influences of winds and currents, and the vessel's residual momentum immediately prior to each downcast. Lateral movement was negligible during the downcasts at Stations RW1, RW3, and RW6, while a southeastward drift at the other stations exceeded 8.5 m. At 17.5m, the lateral movement was greatest Station RW2. The increased vessel movement at Stations RW2, RW4, and RW5 resulted from winds out of the west in combination with current transport toward the southeast.<sup>5</sup> The reduced drift at Stations RW1, RW3, and RW6 arose because the vessel approached these stations from the east, and its residual momentum counteracted the influence of winds and currents.

Regardless of the cause, detailed knowledge of the CTD's movement during downcasts is important for the interpretation of the water-quality measurements. Because the target locations for Stations RW3 and RW4 lie along the ZID boundary (e.g., the red ⊕ symbol in the inset in Figure 2), knowledge of the CTD's location during the downcasts at those stations is especially important in the compliance evaluation. This is because the receiving-water limitations specified in the COP only apply to measurements recorded along or beyond the ZID boundary, where initial mixing is assumed complete.

---

<sup>4</sup> Meteorological and oceanographic conditions include winds, waves, tides, and currents.

<sup>5</sup> Refer to the drogued drifter track shown in Figure 3 later in this report.

During the May 2016 survey, only the mid-depth portion<sup>6</sup> of the data collected at Station RW4 was subject to a compliance assessment because the cast began inside the ZID and traversed the ZID boundary at a depth of 4.5 m as it was transported toward the south. Subsequently, the drift turned toward the west, and the CTD reentered the ZID as it impinged upon the seafloor. Thus, only the data recorded between 4.5 m and 15.5 m at Station RW4 were subject to the compliance analysis. This was the case even though the average location of the CTD data (blue star in the Figure 2 inset) was separated by less than a meter from the target location.

Compliance assessments notwithstanding, measurements acquired within the ZID lend valuable insight into the outfall’s effectiveness at dispersing wastewater. For example, low dilution rates and concentrated effluent throughout the ZID would indicate potentially damaged or broken diffuser ports. Analysis of the outfall’s operation over the past two and a half decades, however, demonstrates that it has maintained a high level of effectiveness in effluent dispersal. In fact, without the occasional measurements recorded within the ZID due to vessel drift, the extremely dilute discharge plume might remain undetected within all the vertical profiles collected during a given survey.

It has not always been possible to determine which measurements were subject to permit limits among hydrocasts near the ZID boundary, however. For example, prior to 1999 and before the advent of DGPS, CTD locations could not be determined with sufficient accuracy to establish whether the average station position was located within the ZID, much less how the CTD was moving laterally during the hydrocast. Because of these navigational limitations, sampling was presumed to occur at a single, imprecisely determined, horizontal location. Federal and state reporting of monitoring data still mandates identification of a single position for all of the CTD data collected at a particular station. Thus, for regulatory reporting, and for consistency with past surveys, the May 2016 survey also identifies a single sampling location for each station. These average station positions are identified by the blue stars in Figure 2, and are listed in Table 2 along with their distances from the diffuser structure.

**Table 2.** Average Position of Vertical Profiles during the May 2016 Survey

Station	Time (PDT)		Latitude	Longitude	Closest Approach	
	Downcast	Upcast			Range <sup>7</sup> (m)	Bearing <sup>8</sup> (°T)
RW1	9:00:09	9:01:28	35° 23.255' N	120° 52.497' W	94.4	16
RW2	9:04:59	9:06:09	35° 23.227' N	120° 52.503' W	42.5	22
RW3	9:09:38	9:10:45	35° 23.208' N	120° 52.499' W	17.9	41
RW4	9:13:46	9:14:59	35° 23.188' N	120° 52.504' W	<b>15.3<sup>9</sup></b>	221
RW5	9:17:27	9:18:40	35° 23.170' N	120° 52.502' W	43.1	195
RW6	9:20:37	9:21:49	35° 23.145' N	120° 52.498' W	86.9	184

<sup>6</sup> Above 5.5 m

<sup>7</sup> Distance from the closest open diffuser port to the average profile location

<sup>8</sup> Angle measured clockwise relative to true north from the closest diffuser port to the average profile location

<sup>9</sup> Some of the CTD measurements were located within the ZID boundary (refer to the inset in Figure 2).

## OCEANOGRAPHIC PROCESSES

The trajectory of a satellite-tracked drogued drifter measured oceanic flow throughout the May 2016 survey (Figure 3). Modeled after the curtain-shade design of Davis et al. (1982) and drogued at mid-depth (7 m), a drifter has been deployed during each of the quarterly water column surveys conducted over the past two decades. In this configuration, the oceanic flow field rather than surface wind dictates the drifter's trajectory, providing a good assessment of the plume's movement after discharge.

During the May 2016 survey, the drifter was deployed near the diffuser structure at 7:28 AM, and was recovered at 9:45 AM at a location 298 m southeast ( $150^{\circ}\text{T}^{10}$ ) of its original release point (red dots in Figure 3). The linear drifter track demonstrated that oceanic current velocity was comparatively consistent throughout the survey. The uniform spacing between the green and black dots in Figure 3, which show the drifter's progress at five- and ten-minute intervals, indicates that flow speed varied little from the average speed of 3.6 cm/s.<sup>11</sup>

At that transport rate, effluent would have experienced a seven-minute residence time within the ZID. However, the drifter trajectory only accurately captures the flow at mid-depth where the drifter's drogue is located. When the water column is highly stratified, as was the case during the May 2016 survey, the flow field often exhibits strong vertical shear where flow direction within the thermocline in the upper water column departs from the mid-depth flow direction measured by the drifter. During the May 2016, the thermocline flow was directed toward the southwest rather than toward the southeast, as measured by the drifter. This vertical difference in flow direction explains why the plume signature measured during the shallow tow extended toward the southwest.<sup>12</sup>

Oceanic flow near the survey area can be influenced by a variety of oceanographic processes, including tidal forcing, and upwelling, and by remote processes, such as large-scale along-shore pressure gradients, or the passing of large eddies embedded within the California Current. At any given time, one or more of these processes may dominate and control the observed flow field. For example, the flood tide that prevailed during the May 2016 survey (Figure 4) tends to induce a weak northeastward (onshore) flow in

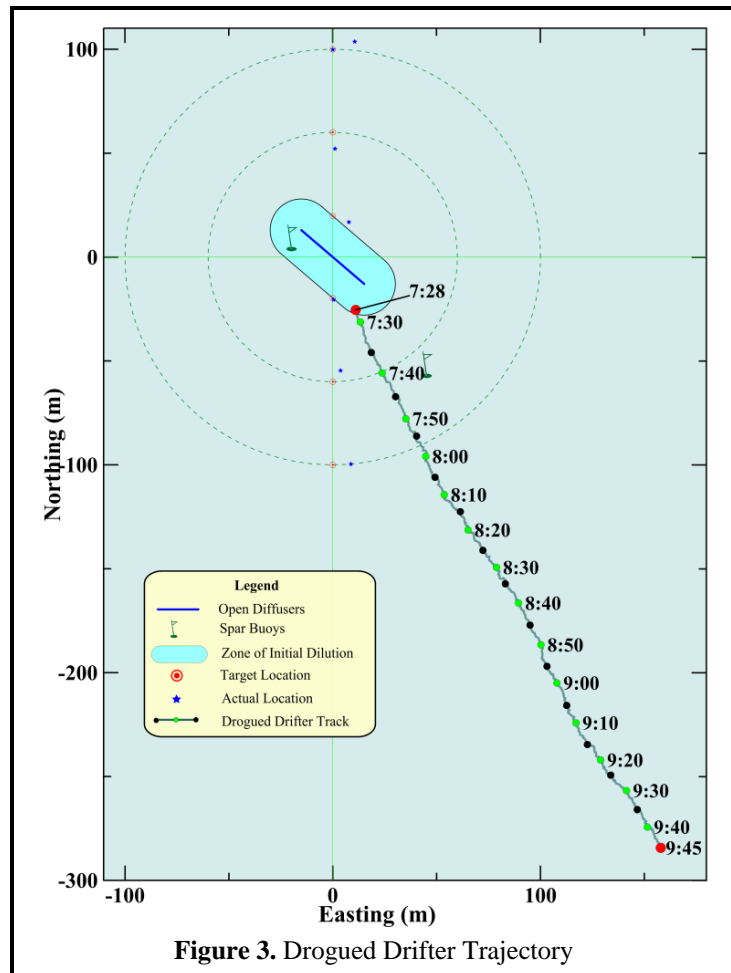


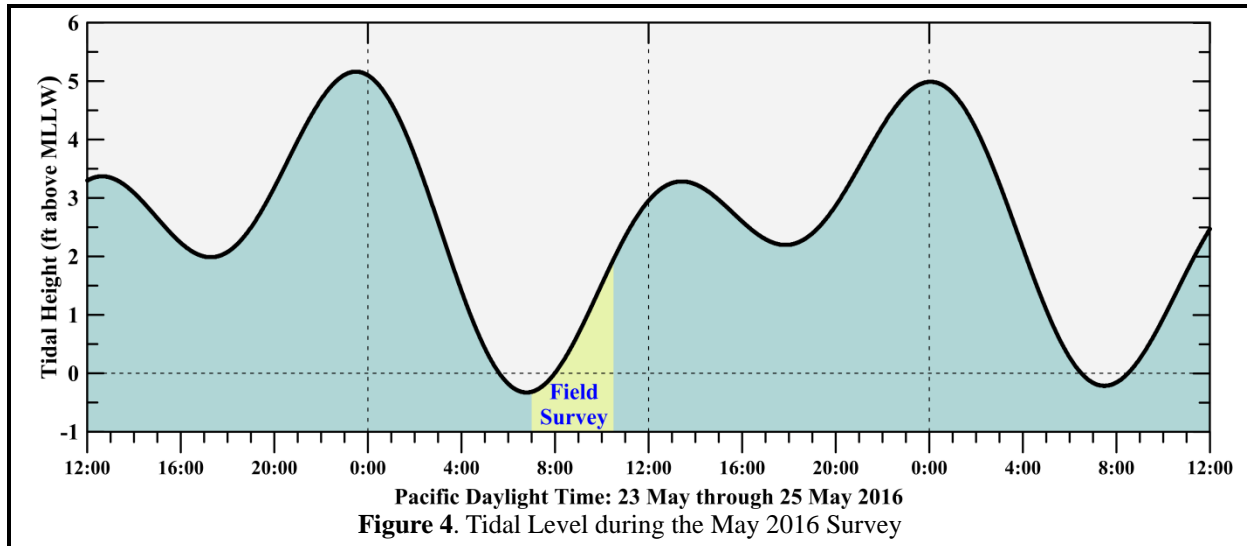
Figure 3. Drogued Drifter Trajectory

<sup>10</sup> Direction measured clockwise relative to true (rather than magnetic) north

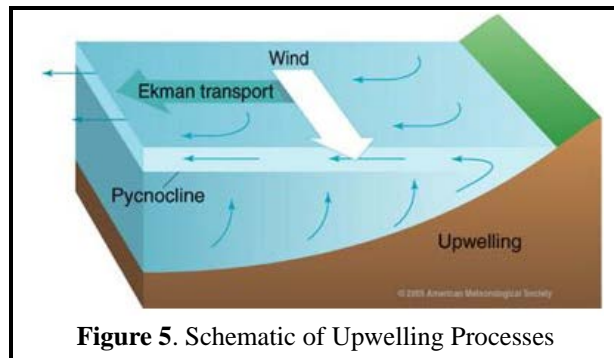
<sup>11</sup> 0.070 kt

<sup>12</sup> See Figure 10abdef later in this report

the survey region. Because this direction is inconsistent with the observed flow, tidal forcing did not materially contribute during the May 2016 survey.



Instead, as is usually the case along this section of coastline, currents within the survey area were largely driven by the prevailing winds out of the northwest. These strong and steady northwesterly winds cause upwelling within the water column and produce a system of vertical countercurrents (Figure 5). In the upper water column, net wind-driven Ekman transport occurs at a 90° angle to the prevailing wind.<sup>13</sup> As a result, warm ocean waters within the surface mixed layer are driven offshore (southwestward) in response to the along-shore winds (toward the southeast). Near the coast, these warm surface waters are replaced by deep, cool, nutrient-rich waters that well up from below. The upwelled waters originate farther offshore and move shoreward along the seafloor as part of the upwelling process. Thus, upwelling establishes a strong vertical shear in flow within the survey area.



The onset of these upwelling-dominated processes begins with a rapid intensification of southeastward-directed winds along the central coast during late March and or early April as shown by the positive (blue) upwelling indices in Figure 6. This transition to more persistent southeastward winds is initiated by the stabilization of a high-pressure field over the northeastern Pacific Ocean. Clockwise winds around this pressure field drive prevailing northwesterly winds along the central California coast. The May 2016 survey was conducted after the onset of this spring transition and when upwelling conditions were well established (see the inset in Figure 6).

The nutrient-rich seawater that is brought to the sea surface near the coast by upwelling enables phytoplanktonic blooms that are the foundation of the productive marine fishery found along the central California coast. The vertical counterflow associated with persistent upwelling conditions also enhances vertical stratification of the water column. The influx of cold dense water at depth produces a shallow thermocline (<10 m) that is commonly maintained throughout summer and into fall.

<sup>13</sup> <http://oceanmotion.org/html/background/upwelling-and-downwelling.htm>

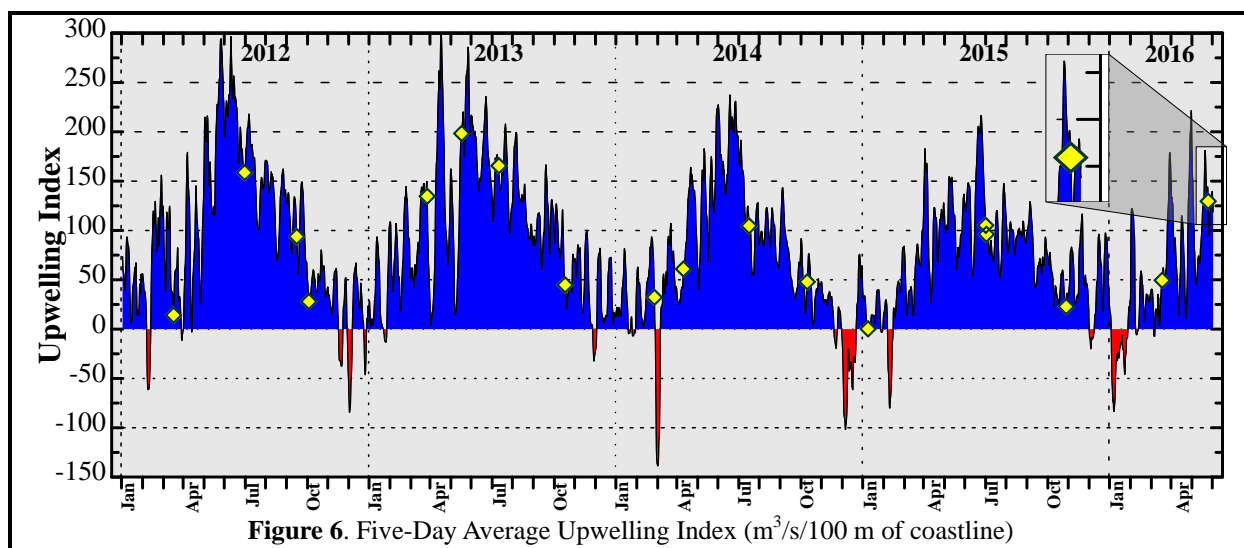


Figure 6. Five-Day Average Upwelling Index ( $\text{m}^3/\text{s}/100 \text{ m}$  of coastline)

Some degree of upwelling is almost always present during offshore surveys (yellow diamonds in Figure 6). During winter, upwelling is typically weak, and occasionally downwelling events, indicated by the negative (red shaded) indices in Figure 6, occur when passing storms temporarily reverse the normal wind pattern and drive surface waters shoreward. As the surface waters approach the coastline, they downwell, producing nearly uniform seawater properties throughout the water column.

Because the May 2016 survey took place when upwelling was well underway, strong upwelling winds were present (see the inset showing the last yellow diamond in Figure 6). These winds produced a pattern of sea surface temperatures indicative of upwelling processes within the central-coast region. This pattern was captured by the satellite image shown on the cover of this report. The image was recorded by infrared sensors on one of NOAA's polar orbiting satellites during a period of relatively cloudless skies on the day prior to the survey. Cooler upwelled water is visually apparent along the entire south-central coastline (purple and dark blue shading). Jets of upwelled water often extend offshore at major promontories, such as the one extending offshore Point Piedras Blancas at the time of the May 2016 survey.

However, various swirls and eddies are also apparent in the surface temperature pattern, suggesting additional flow complexity. Nevertheless, southwestward (offshore) surface flow was reflected in the effluent plume's transport captured by the shallow tow survey. Additionally, the overall surface temperature distribution shown in the satellite image was consistent with strong upwelling, as reflected by the  $5^\circ\text{C}$  cross-shore thermal contrast. Thus, the May 2016 survey captured the advanced stages of upwelling, and as a result, the water column was strongly stratified. As described later in this report, however, the strength of the stratification was not sufficient to prevent the buoyant plume from reaching the sea surface. When buoyancy forces within the effluent plume are weaker, strong stratification can trap the rising effluent plume beneath the sea surface, and curtail the initial dilution process.

## METHODS

The 38 ft F/V *Bonnie Marietta*, owned and operated by Captain Mark Tognazzini of Morro Bay, served as the survey vessel on Tuesday, 24 May 2016. Douglas Coats of Marine Research Specialists (MRS) supervised scientific operations as Chief Scientist, and provided data-acquisition and navigational support during the survey. He also assisted with the deployment and recovery of the CTD and drifter, and collected meteorological measurements at each station. Crewmember William Skok managed deck operations and collected the Secchi depth measurements at each station.

### *Auxiliary Measurements*

Auxiliary measurements and observations were collected during the vertical water-column profiling conducted at each of the six stations. Standard observations of weather and sea conditions, and beneficial uses, were augmented by visual inspection of the sea surface for floating particulates, oil sheens, and discoloration potentially related to effluent discharge. Other auxiliary measurements collected at each station included wind speeds and air temperatures measured with a handheld Kestrel® 2000 Thermo-Anemometer, and oceanic flow measurements made throughout the survey area using a drogued drifter.

Additionally, at all six stations, a Secchi disk was lowered through the water column to determine its depth of disappearance. Secchi depths provide a visual measure of near-surface turbidity or water clarity. The depth of disappearance is inversely proportional to the average amount of organic and inorganic material suspended along a line of sight in the upper water column. As such, Secchi depths measure natural light penetration, which can be limited by increased suspended particulate loads from plankton blooms, onshore runoff, seafloor sediment resuspension, and wastewater discharge. They are also biologically meaningful because the depth of the euphotic zone, where most oceanic photosynthesis occurs, is limited to approximately twice the Secchi depth.

### *Instrumental Measurements*

A Sea Bird Electronics SBE-19plusV2 Seacat CTD instrument package collected measurements of conductivity, temperature, light transmittance, dissolved oxygen (DO), pH, and pressure during the May 2016 survey. The six seawater properties used to assess receiving-water quality in this report were derived from the continuously recorded output from the CTD's probes and sensors. Although pressure-housing limitations confine the CTD to depths less than 680 m (Table 3), this is well beyond the maximum depth of the deepest station in the outfall survey. The entire CTD was returned to the factory in January 2015 for full calibration and servicing. The transmissometer and DO probe were returned to the manufacturer in January 2016 for further servicing, repair, and calibration.

**Table 3. CTD Specifications**

<b>Component</b>	<b>Units</b>	<b>Range</b>	<b>Accuracy</b>	<b>Resolution</b>
Housing (19p-1a; Acetron Plastic)	m	0 to 680	—	—
Pump (SBE 5P)	—	—	—	—
Pressure (19p-2h; Strain-Gauge)	dBar	0 to 680	±1.7	± 0.10
Conductivity	Siemens/m	0 to 9	± 0.0005	± 0.00005
Salinity	‰	0 to 58	± 0.004	± 0.0004
Temperature	°C	-5 to 35	± 0.005	± 0.0001
Transmissivity (WETLabs C-Star) <sup>14</sup>	%	0 to 100	± 0.3	± 0.03
Oxygen (SBE 43)	% Saturation	0 to 120	± 2	—
pH (SBE 18)	pH	0 to 14	± 0.1	—

The precision and accuracy of the various probes, as reported in manufacturer's specifications, are listed in Table 3. Salinity (‰) was calculated from conductivity measurements reported in units of Siemens/m. Density was derived from contemporaneous temperature (°C) and salinity data, and was expressed as 1000 times the specific gravity minus one, which is a unit of sigma-T ( $\sigma_t$ ).

<sup>14</sup> 25-cm path length of red (650 nm) light

Assessments of all three of the physical parameters (salinity, temperature, and density) helped determine the lateral extent of the effluent plume during the towing phase of the survey. Additionally, during the vertical-profiling phase, they quantified layering, or vertical stratification and stability of the water column, which determines the behavior and dynamics of the effluent as it mixes with seawater within and beyond the ZID. Data on the three remaining seawater properties, light transmittance (water clarity), hydrogen-ion concentration (acidity/alkalinity – pH), and dissolved oxygen (DO), further characterized the receiving waters, and were used to assess compliance with water-quality criteria. Light transmittance was measured as a percentage of the initial intensity of a transmitted beam of light detected at the opposite end of a 0.25-m path. Transmissivity readings are reported relative to 100% transmission in air, so the maximum theoretical transmission in (pure) water is expected to be 91.3%.

Before beginning the mid-depth tow survey at 7:38 AM, the CTD was deployed beneath the sea surface for nine minutes as the vessel was positioned to begin the first transect. Prior to deployment, the CTD package had been configured for horizontal towing with forward-looking probes. The protective cage around the CTD was fitted with a horizontal stabilizer wing and a depth-suppression weight was added to the towline to achieve near constant-depth tows.

Eight transects of mid-depth data were collected at an average depth of 9.0 m and an average speed of 1.60 m/s over the span of 35 minutes (blue-green lines in Figure 7). Subsequently, at 8:15 AM, eight additional passes were made with the CTD at an average depth of 3.5 m (orange lines). During this 30-minute shallow tow, vessel speed averaged 1.64 m/s. At the observed towing speeds and the 4 Hz sampling rate, at least 2.4 CTD measurements were collected for each meter traversed. This complies with the NPDES discharge permit requirement for minimum horizontal resolution of at least one sample per meter during at least five passes around and across the ZID at two separate depths, one within the surface mixed layer and one at mid-depth within the thermocline.

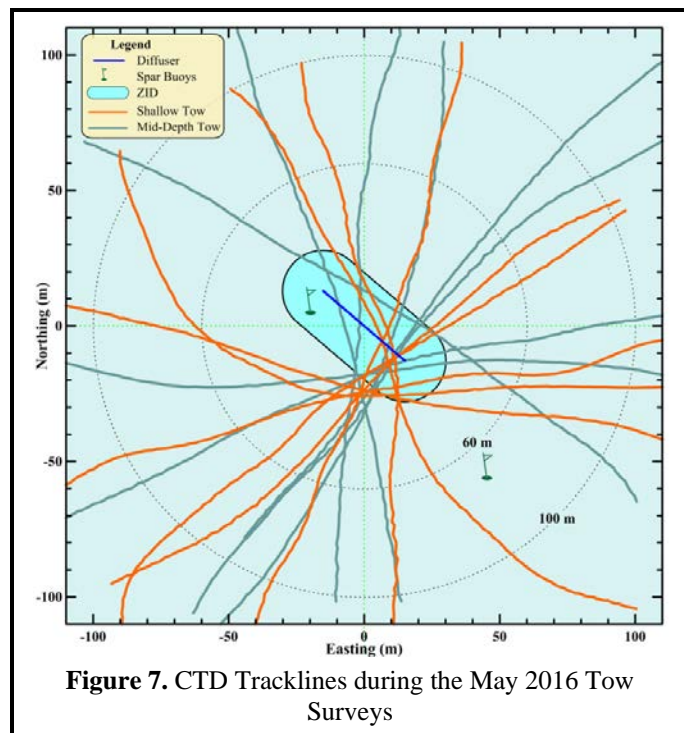


Figure 7. CTD Tracklines during the May 2016 Tow Surveys

Contemporaneous navigation fixes recorded onboard the survey vessel were adjusted for CTD setback and aligned with time stamps on the internally recorded CTD data. The resulting data for the six seawater properties were then processed to produce horizontal maps within the upper and sub-thermocline portions of the water column.<sup>15</sup>

At 8:45 AM, following completion of the last shallow transect, the CTD package was brought aboard the survey vessel and reconfigured for vertical profiling. The CTD was redeployed at 8:54 AM, and was held beneath the surface for six minutes as the vessel was repositioned over Station RW1. The CTD was then raised to within 0.5 m of the sea surface and profiling commenced. The CTD was lowered at a continuous rate of speed to the seafloor. Measurements at all six stations were collected during a single deployment of the CTD package by towing it below the ocean surface while transiting between adjacent stations.

<sup>15</sup> Figures 9 and 10 later in this report

### *Quality Control*

During the vertical-profiling and horizontal-towing phases of the survey, real-time data were monitored for completeness and range acceptability. Although real-time monitoring indicated the recorded properties were complete and within acceptable coastal seawater ranges,<sup>16</sup> subsequent post-processing revealed several events that impacted portions of the data, resulting in the adjustment or exclusion of these data prior to initiating the compliance analysis. Specifically, review of the tow data revealed that the CTD changed depth when the vessel executed a turn at the end of each transect. These vertical offsets in CTD depth are induced by changes in vessel speed and direction that are instituted to realign the vessel between each transect. Because of the complex interaction between turn radius, vessel speed, and CTD depth, the CTD's target depth cannot always be maintained at these times.

Because the discharge-related anomalies used in the compliance analysis are identified by comparing the amplitudes of measurements acquired at the same depth level, the ability to resolve anomalies with statistical certainty is compromised when data from different depth levels are combined in the horizontal maps. This is particularly true whenever the water column is strongly stratified, as was the case during the May 2016 survey.

However, the exclusion of portions of tow data that were collected when the vessel was turning did not adversely affect the compliance analysis because all transects had straight sections that were long enough to fully encompass the 100-m survey area surrounding the diffuser structure. Specifically, the tow data that were included in the compliance analysis, shown by the solid orange and blue-green lines in Figure 7, met the permit monitoring requirement of at least five passes near the diffuser structure at each tow depth.

## **RESULTS**

The second-quarter receiving-water survey was conducted on the morning of Tuesday, 24 May 2016. The receiving-water survey commenced at 7:28 AM with the deployment of the drogued drifter. Over the course of the ensuing two hours, offshore observations and measurements were collected as required by the NPDES monitoring program. The survey ended at 9:45 AM with the retrieval of the drogued drifter. Collection of required visual observations of the sea surface was generally unencumbered throughout the survey.

### *Auxiliary Observations*

On the morning of 24 May 2016, skies were overcast, with a sustained light onshore breeze out of the southwest. Auxiliary observations were collected beginning at 9:27 AM, after completion of the vertical profiling phase of the survey. During the subsequent 15 minutes, each station was re-occupied beginning with Station RW6, and sequentially progressing toward the north. During that time, winds shifted from out of the south to a more west-southwesterly direction. Average wind speeds, calculated over one-minute intervals, decreased from 3.6 kt to 2.2 kt (Table 4). Peak wind speeds declined from 4.3 kt to 3.0 kt. A swell out of the northwest had a significant wave height of two-to-three feet. Air temperatures remained fairly constant and averaged 14.8°C, which was slightly warmer than the 13.0°C sea surface temperature.

---

<sup>16</sup> Field sampling protocols employed during the survey generally followed the field operations manual for the Southern California Bight Study (SCBFMC 2002), which includes CTD cast-acceptability ranges listed in Table 2 of the manual.

**Table 4.** Standard Meteorological and Oceanographic Observations

Station	Location <sup>17</sup>		Diffuser Distance (m)	Time (PDT)	Air (°C)	Cloud Cover (%)	Wind Avg (kt)	Wind Max (kt)	Wind Dir (from) (°T)	Swell Ht/Dir (ft/°T)	Secchi Depth (m)
	Latitude	Longitude									
RW1	35° 23.252' N	120° 52.502' W	86.0	9:41:49	15.0	40	2.2	3.0	240	2-3 NW	4.5
RW2	35° 23.233' N	120° 52.498' W	55.0	9:39:00	14.2	50	2.6	3.4	230	2-3 NW	4.5
RW3	35° 23.210' N	120° 52.503' W	16.8	9:35:44	14.4	60	3.0	3.8	225	2-3 NW	4.0
RW4	35° 23.190' N	120° 52.503' W	11.6	9:33:00	15.4	70	2.9	3.9	198	2-3 NW	4.0
RW5	35° 23.165' N	120° 52.503' W	52.3	9:29:22	14.2	75	2.9	3.9	240	2-3 NW	4.0
RW6	35° 23.144' N	120° 52.500' W	88.7	9:26:35	15.3	80	3.6	4.3	175	2-3 NW	4.0

There was no evidence of floating particulates, oil sheens, or any discoloration of the sea surface associated with the presence of wastewater constituents. There was no other visual indication of the presence of the discharge plume at or beneath the sea surface during the survey. Ambient light penetration through the water column was limited by an increased density of planktonic organisms within the thermocline in the upper water column. During upwelling, nutrients carried upward into the euphotic zone are assimilated by phytoplankton, whose populations increase and, along with their associated zooplanktonic herbivores; their elevated densities reduce the transmittance of ambient light. At stations unaffected by the discharge during the May 2016 survey, plankton-induced increases in turbidity spanned a depth range between 3 m and 7 m.

Because of this layer of increased turbidity, the Secchi disk disappeared between a depth of between 4 m and 4.5 m as it was lowered through the water column at each station during the May 2016 survey (Table 4). The measured Secchi depth indicates that an 8.5 m euphotic zone was present during the survey, and that ambient light only penetrated through the upper half of the water column and did not reach the base of the thermocline where the mid-depth tow was conducted.

Because the Secchi-depth measurements were nearly the same at all the stations, near-surface water clarity was not impacted by the presence of the plume, at least at the locations where the Secchi depth was measured. If anything, shallow measurements within the plume would be expected to increase Secchi depth because the rising effluent plume carried relatively clear deeper water into the shallow more-turbid mixed layer. Consistent with the relatively invariant Secchi depths, there was no visual evidence of the plume signature at the sea surface at any time during the survey. Similarly, no evidence of floating particulates, oil sheens, or any discoloration of the sea surface was visually apparent that might be related to the presence of wastewater constituents

Communication with plant personnel and subsequent review of effluent discharge properties on the day of the survey, confirmed that the treatment process was performing well at time of the survey. The 0.759 million gallons of effluent discharged on 24 May had a temperature of 22°C, a suspended-solids concentration of 25.6 mg/L, and a pH of 7.6. The 4.2 mg/L oil and grease concentration measured within effluent discharged on the day of the survey was below the method quantification threshold. The biochemical oxygen demand (BOD) of the effluent measured two days after the survey, on 26 May, was 49 mg/L.

<sup>17</sup> Locations are the vessel positions at the time the Secchi depths were measured. These depart from the CTD profile locations listed in Table 2 because they were collected after completion of the CTD profiling.

### *Instrumental Observations*

Data collected during vertical profiling were processed in accordance with standard procedures (SCCWRP 2002), and are collated within 0.5-m depth intervals in Table 5. Data collected during the May 2016 survey reflect strongly stratified conditions within Estero Bay indicative of a fully developed coastal upwelling phenomenon (refer to the inset in Figure 6).

Upwelling of varying intensity occurs most of the year along the central California coast, with the strongest upwelling winds beginning in March or April and extending through the summer. The intensity of upwelling tends to decline into fall, although pulses of sustained northwesterly winds still occur. An intense upwelling event results in the rapid influx of dense, cold, saline water at depth and leads to a sharp thermocline, halocline, and pycnocline where temperature, salinity, and density change rapidly over a small vertical distance. Under these highly stratified conditions, isotherms crowd together to form a density interface that inhibits the vertical exchange of nutrients and other water properties, traps the effluent plume at depth, and reduces the initial dilution of the effluent plume.

Although winds were light on the day of the survey, strong sustained northwesterly winds prevailed in the days prior to the survey, resulting in intense upwelling. Consequently, vertical profiles of seawater properties measured at the northern stations (RW1, RW2, and RW3), which were unaffected by the discharge, exhibit a marked vertical transition beneath a 2-m surface mixed layer (Figure 8abc). This transition zone extended to a depth of 7 m, and separated the surface mixed layer from a deep watermass containing more uniform seawater properties. Within this transition zone, seawater properties exhibited steadily increasing or decreasing values with depth that are determined by well-established physicochemical processes within ocean waters. In particular, temperature (red lines), DO (dark blue lines), pH (olive-colored lines) steadily decrease with increasing depth. These decreases are mirrored by a halocline and pycnocline, where salinity (green lines) and density (black lines) increase with depth.

These vertical changes reflect the transition to a colder, saltier, nutrient-rich but oxygen-poor watermass that migrated shoreward along the seafloor as part of the upwelling process. This offshore watermass moved shoreward to replace nearshore surface waters that were driven offshore by the prevailing northwesterly winds (Figure 5). The seawater properties of this deep watermass originate within the northward-flowing Davidson undercurrent that carried more saline and less oxygenated waters out of the Southern California Bight and northward along the central California coast. Because this deep offshore watermass had not been in recent direct contact with the atmosphere, biotic respiration and decomposition had depleted its DO levels (dark blue lines). Additionally, at depth, biotic respiration and decomposition produced carbon dioxide (CO<sub>2</sub>), and in its dissolved state, the increased concentration of carbonic acid appears as a concomitant reduction in pH (olive-colored lines). Similarly, the slightly increased salinity observed near the seafloor (green lines) originates with the saltier seawater transported from the southern California bight.

Meanwhile, within the euphotic zone, nutrient-rich seawater brought to the sea surface by the recent upwelling facilitated phytoplankton blooms that produced oxygen, consumed carbon dioxide (increasing pH), and decreased water clarity (light blue lines). The presence of plankton within the transition zone (thermocline) caused a 5.2% decrease in transmissivity compared to the deep water mass.

Table 5. Vertical Profile Data Collected on 24 May 2016

Depth (m)	Temperature (°C)						Salinity (‰)					
	RW-1	RW-2	RW-3	RW-4	RW-5	RW-6	RW-1	RW-2	RW-3	RW-4	RW-5	RW-6
0.5	13.125	12.733				13.191	33.550	33.528				33.552
1.0	13.104	12.730	12.662	11.495	13.070	13.087	33.548	33.532	33.528	33.439	33.546	33.547
1.5	13.083	12.716	12.419	11.487	12.936	12.917	33.548	33.532	33.506	33.439	33.534	33.534
2.0	13.007	12.564	12.257	11.478	12.741	12.446	33.545	33.519	33.501	33.439	33.525	33.487
2.5	12.522	12.318	12.127	11.497	12.358	12.059	33.504	33.504	33.500	33.446	33.472	33.488
3.0	12.094	12.167	12.061	11.489	11.927	11.895	33.489	33.498	33.502	33.443	33.434	33.491
3.5	12.076	12.058	12.036	11.397	11.594	11.789	33.499	33.498	33.507	33.437	33.416	33.481
4.0	12.019	11.968	11.931	11.352	11.501	11.636	33.504	33.505	33.507	33.435	33.423	33.455
4.5	11.877	11.856	11.834	11.341	11.436	11.496	33.508	33.510	33.515	33.439	33.430	33.448
5.0	11.779	11.753	11.729	11.354	11.402	11.455	33.519	33.515	33.520	33.443	33.438	33.461
5.5	11.665	11.705	11.686	11.344	11.375	11.425	33.521	33.521	33.523	33.452	33.449	33.470
6.0	11.550	11.647	11.676	11.344	11.371	11.415	33.522	33.522	33.526	33.457	33.464	33.481
6.5	11.459	11.534	11.661	11.339	11.379	11.410	33.528	33.522	33.527	33.463	33.480	33.495
7.0	11.429	11.461	11.630	11.341	11.394	11.394	33.531	33.527	33.528	33.471	33.504	33.514
7.5	11.424	11.429	11.587	11.346	11.395	11.368	33.533	33.529	33.527	33.482	33.525	33.531
8.0	11.405	11.411	11.507	11.371	11.380	11.346	33.534	33.532	33.525	33.529	33.535	33.536
8.5	11.394	11.393	11.453	11.357	11.360	11.310	33.536	33.534	33.530	33.539	33.538	33.537
9.0	11.373	11.375	11.421	11.328	11.332	11.288	33.537	33.536	33.530	33.541	33.540	33.541
9.5	11.370	11.357	11.404	11.319	11.314	11.267	33.538	33.539	33.533	33.542	33.541	33.544
10.0	11.366	11.352	11.394	11.308	11.295	11.260	33.539	33.540	33.535	33.543	33.542	33.545
10.5	11.362	11.344	11.376	11.296	11.273	11.259	33.540	33.541	33.536	33.544	33.544	33.547
11.0	11.345	11.341	11.352	11.282	11.260	11.258	33.541	33.541	33.538	33.544	33.545	33.547
11.5	11.344	11.342	11.344	11.273	11.249	11.254	33.542	33.542	33.539	33.545	33.547	33.548
12.0	11.343	11.337	11.343	11.267	11.226	11.247	33.543	33.542	33.541	33.546	33.548	33.549
12.5	11.340	11.333	11.336	11.263	11.223	11.228	33.543	33.543	33.542	33.547	33.549	33.549
13.0	11.340	11.330	11.333	11.257	11.224	11.225	33.543	33.543	33.542	33.548	33.550	33.550
13.5	11.337	11.331	11.332	11.242	11.226	11.211	33.543	33.544	33.543	33.548	33.550	33.551
14.0	11.337	11.336	11.332	11.237	11.226	11.198	33.544	33.544	33.543	33.549	33.550	33.551
14.5	11.334	11.340	11.335	11.213	11.223	11.197	33.545	33.544	33.543	33.550	33.551	33.552
15.0	11.334	11.344	11.342	11.214	11.223	11.198	33.545	33.544	33.544	33.552	33.551	33.552
15.5		11.344	11.347	11.225	11.226	11.198		33.544	33.544	33.552	33.551	33.552
16.0				11.224						33.551		

Table 5. Vertical Profile Data Collected on 24 May 2016 (continued)

Depth (m)	Density ( $\sigma_t$ )						pH					
	RW-1	RW-2	RW-3	RW-4	RW-5	RW-6	RW-1	RW-2	RW-3	RW-4	RW-5	RW-6
0.5	25.245	25.309				25.233	8.086	8.094				8.101
1.0	25.248	25.309	25.319	25.471	25.253	25.250	8.084	8.093	8.099	7.974	8.099	8.102
1.5	25.251	25.312	25.349	25.472	25.270	25.274	8.084	8.093	8.101	7.975	8.099	8.101
2.0	25.264	25.332	25.377	25.474	25.301	25.329	8.085	8.094	8.101	7.973	8.097	8.100
2.5	25.328	25.367	25.400	25.476	25.334	25.404	8.083	8.098	8.096	7.974	8.083	8.097
3.0	25.398	25.391	25.415	25.475	25.387	25.437	8.086	8.096	8.090	7.975	8.066	8.090
3.5	25.409	25.412	25.423	25.487	25.434	25.449	8.079	8.088	8.088	7.974	8.038	8.076
4.0	25.423	25.434	25.442	25.494	25.457	25.457	8.076	8.081	8.086	7.965	8.006	8.056
4.5	25.453	25.459	25.467	25.498	25.474	25.477	8.077	8.076	8.076	7.956	7.992	8.031
5.0	25.480	25.482	25.490	25.500	25.487	25.495	8.076	8.065	8.068	7.953	7.983	8.006
5.5	25.503	25.496	25.501	25.508	25.500	25.508	8.062	8.056	8.059	7.952	7.976	7.995
6.0	25.525	25.508	25.505	25.512	25.512	25.518	8.051	8.048	8.052	7.953	7.972	7.988
6.5	25.546	25.528	25.509	25.518	25.524	25.529	8.037	8.034	8.049	7.953	7.970	7.986
7.0	25.554	25.545	25.515	25.523	25.539	25.548	8.019	8.019	8.046	7.952	7.971	7.987
7.5	25.557	25.552	25.522	25.531	25.556	25.565	8.009	8.008	8.041	7.953	7.976	7.986
8.0	25.561	25.558	25.535	25.563	25.566	25.573	8.001	8.001	8.035	7.954	7.982	7.984
8.5	25.564	25.563	25.549	25.574	25.572	25.581	7.997	7.996	8.027	7.961	7.983	7.979
9.0	25.569	25.568	25.555	25.580	25.579	25.588	7.996	7.991	8.014	7.968	7.981	7.973
9.5	25.570	25.573	25.561	25.583	25.583	25.593	7.993	7.982	8.010	7.966	7.977	7.968
10.0	25.572	25.576	25.564	25.585	25.587	25.596	7.989	7.977	8.001	7.965	7.974	7.963
10.5	25.574	25.577	25.568	25.588	25.593	25.597	7.986	7.975	7.996	7.963	7.969	7.956
11.0	25.578	25.578	25.574	25.591	25.596	25.598	7.981	7.971	7.992	7.961	7.965	7.954
11.5	25.579	25.579	25.576	25.594	25.599	25.599	7.976	7.970	7.985	7.959	7.961	7.952
12.0	25.579	25.580	25.577	25.596	25.604	25.601	7.974	7.968	7.980	7.955	7.956	7.949
12.5	25.580	25.581	25.579	25.597	25.606	25.605	7.972	7.967	7.977	7.951	7.951	7.946
13.0	25.580	25.582	25.580	25.598	25.606	25.606	7.970	7.964	7.974	7.949	7.947	7.942
13.5	25.581	25.582	25.581	25.602	25.606	25.609	7.966	7.963	7.971	7.945	7.943	7.940
14.0	25.581	25.581	25.581	25.603	25.606	25.612	7.963	7.962	7.969	7.942	7.944	7.938
14.5	25.582	25.581	25.581	25.608	25.607	25.613	7.959	7.959	7.966	7.937	7.942	7.935
15.0	25.582	25.580	25.580	25.610	25.607	25.613	7.956	7.957	7.962	7.932	7.937	7.935
15.5		25.580	25.579	25.607	25.607	25.613		7.955	7.955	7.926	7.930	7.933
16.0				25.607						7.922		

Table 5. Vertical Profile Data Collected on 24 May 2016 (continued)

Depth (m)	Dissolved Oxygen (mg/L)						Transmissivity (%)					
	RW-1	RW-2	RW-3	RW-4	RW-5	RW-6	RW-1	RW-2	RW-3	RW-4	RW-5	RW-6
0.5	9.004	9.261				9.275	82.865	83.141				82.203
1.0	8.980	9.227	9.346	7.571	9.149	9.158	83.061	83.033	82.235	82.122	82.902	82.906
1.5	8.919	9.265	9.353	7.575	9.009	9.160	82.872	83.478	81.920	82.015	82.821	82.835
2.0	8.996	9.358	9.281	7.599	8.294	9.064	82.734	83.341	81.125	82.155	82.304	81.963
2.5	9.099	9.273	9.247	7.542	7.605	8.853	82.578	82.706	80.292	82.025	81.746	81.059
3.0	9.115	9.143	9.186	7.304	7.503	8.510	82.282	82.335	79.666	82.138	81.896	79.065
3.5	9.093	9.014	8.986	7.226	7.498	7.911	81.185	80.847	78.949	82.133	82.516	77.420
4.0	8.813	8.841	8.763	7.243	7.463	7.651	80.330	79.658	78.575	82.638	82.781	78.565
4.5	8.680	8.694	8.631	7.277	7.423	7.654	79.996	79.463	79.074	82.796	82.410	81.556
5.0	8.423	8.578	8.576	7.297	7.391	7.629	79.365	78.718	78.715	82.860	82.650	82.178
5.5	8.097	8.326	8.562	7.293	7.414	7.666	78.943	78.615	79.102	82.932	82.684	82.420
6.0	7.905	7.999	8.457	7.282	7.534	7.658	79.063	79.403	79.947	82.856	83.199	82.700
6.5	7.835	7.891	8.361	7.330	7.669	7.649	78.870	79.214	79.276	83.039	82.663	82.695
7.0	7.815	7.807	8.193	7.389	7.682	7.608	81.495	80.863	78.858	83.470	83.212	83.225
7.5	7.758	7.753	7.936	7.601	7.651	7.557	82.570	82.429	78.964	83.312	83.395	83.562
8.0	7.726	7.688	7.882	7.486	7.587	7.414	83.000	82.948	78.793	83.720	83.334	83.780
8.5	7.662	7.578	7.787	7.392	7.464	7.300	83.060	83.084	80.809	83.623	84.159	84.525
9.0	7.661	7.487	7.741	7.362	7.424	7.232	83.385	83.743	82.677	83.791	83.858	84.965
9.5	7.612	7.470	7.698	7.321	7.344	7.200	84.438	83.999	83.680	84.504	84.465	85.285
10.0	7.578	7.425	7.591	7.279	7.270	7.173	84.828	84.598	83.793	84.629	84.527	85.387
10.5	7.484	7.425	7.529	7.219	7.225	7.151	84.073	84.382	83.646	84.583	84.815	85.426
11.0	7.457	7.429	7.482	7.186	7.166	7.126	84.092	84.206	83.827	84.952	85.288	85.813
11.5	7.432	7.389	7.431	7.135	7.061	7.049	84.261	84.557	84.271	84.856	85.526	85.530
12.0	7.392	7.379	7.393	7.103	7.047	6.997	84.061	84.561	84.582	85.397	85.554	85.714
12.5	7.394	7.336	7.381	7.060	7.052	6.992	84.315	84.506	84.508	85.347	85.374	85.886
13.0	7.323	7.343	7.374	7.005	7.035	6.933	84.383	84.981	84.804	85.094	86.369	86.215
13.5	7.257	7.334	7.352	6.946	7.008	6.932	84.723	84.827	85.183	85.173	85.770	85.964
14.0	7.104	7.294	7.313	6.760	6.907	6.915	84.451	84.356	84.760	85.177	85.498	86.706
14.5	7.046	7.229	7.264	6.749	6.862	6.899	84.335	84.641	84.737	85.445	85.334	86.892
15.0	7.168	7.268	7.268	6.731	6.849	6.899	85.234	84.978	86.325	85.621	86.188	86.698
15.5		7.266	7.317	6.745	6.851	6.925		84.502	87.345	86.125	86.493	86.498
16.0				6.737						85.988		

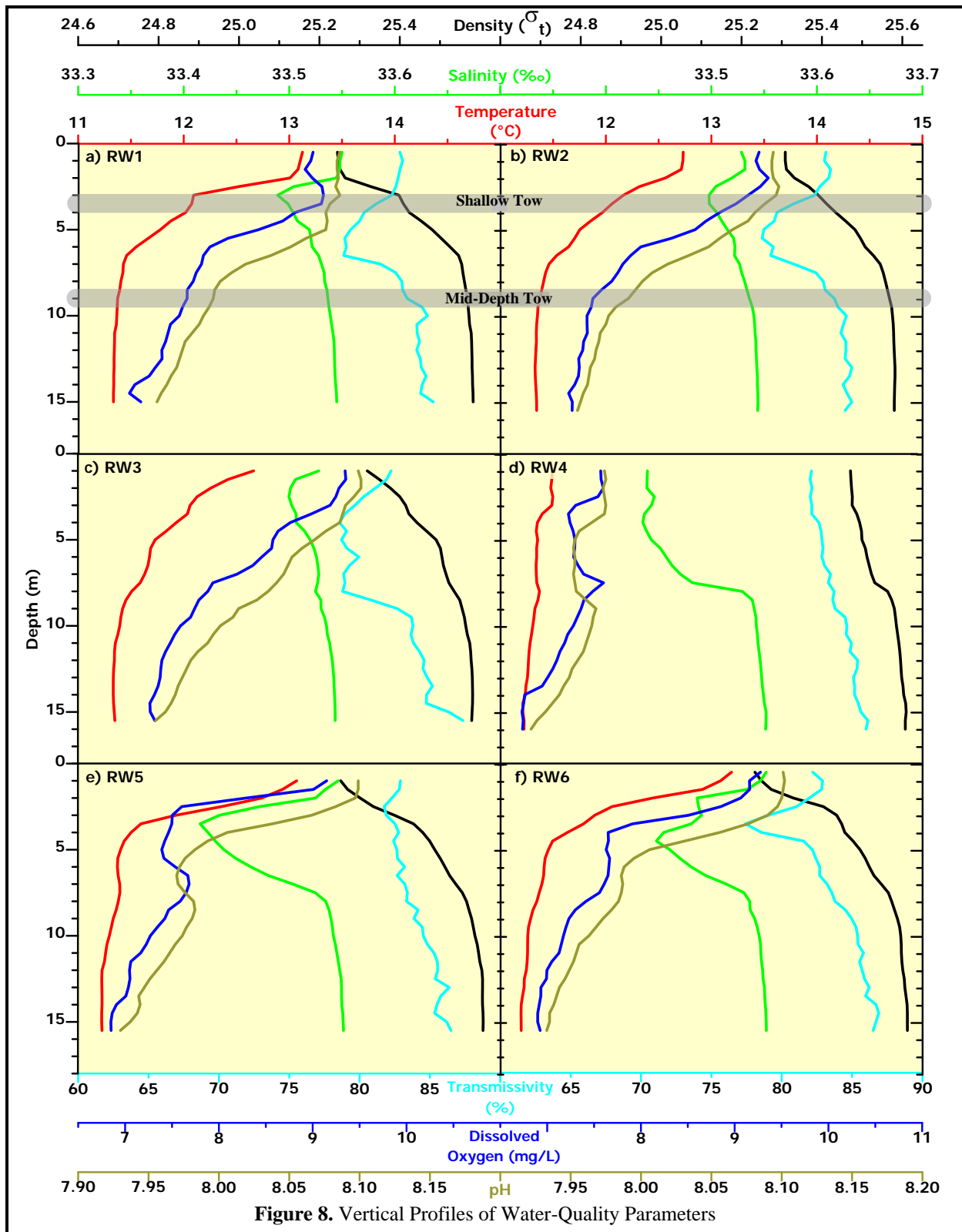


Figure 8. Vertical Profiles of Water-Quality Parameters

The tow surveys delineated the low-salinity signature of the buoyant effluent plume in localized areas south of the diffuser structure (Figures 9b and 10b). How As the rising effluent plume was transported to the south by the prevailing flow field, it conspicuously altered the ambient vertical structure discussed above. Immediately south of the diffuser structure, vertical profiles at Station RW4 (Figure 8d) were nearly uniform as a result of the upward transport of deep seawater properties within the rising plume. The absence of a distinct transition zone indicates that the plume had risen to the sea surface, and did not become trapped at depth, as is often the case within a strongly stratified water column. Farther south, at Stations RW5 and RW6 (Figure 8ef), the plume only carried deep ambient seawater properties to a depth of 4 m, where it noticeably compressed the near-surface transition zone.

However, because the mid-depth tow was conducted at a depth within the relatively uniform deep watermass (bottom shaded line in Figure 8ab), upward transport of ambient seawater entrained by the discharge plume near the seafloor did not provide a sharp contrast with surrounding seawater at the 9-m tow depth. Consequently, there were no obvious anomalies in temperature, transmissivity, DO, and pH (Figure 9adef) that coincided with the mid-depth salinity and density anomalies (Figure 9bc). The markedly reduced density within the plume (Figure 9c) indicates that the plume was highly buoyant at that point, and would continue to mix rapidly during its subsequent ascent through the rest of the water column. Thus, the mid-depth tow captured the early stages of the initial dilution process. At that time, the plume was of limited lateral extent, and largely confined to the ZID.

The shallow tow captured a later stage of the dilution process after the plume had risen to a depth well within the transition zone (upper shaded line in Figure 8ab). At that point, a weaker salinity anomaly delineated a more-widespread plume signature extending toward the southwest (Figure 10b). However, in contrast to the mid-depth tow, no obvious density reduction coincided spatially with the salinity anomaly (Figure 10c). The plume's near-neutral buoyancy indicates that the initial dilution process was largely complete at that point. However, now that the plume had transported the deep seawater characteristics upward into the transition zone, they created a sharp contrast with the surrounding ambient seawater. As a result, clearly defined reductions in temperature, DO, and pH (Figure 10aef) delineated the plume's location while increased transmissivity was found in the same general location (Figure 10d).

The decreased temperature and increased transmissivity (less turbidity) are particularly diagnostic of anomalies created by the entrainment of bottom seawater; they could not have been generated by the presence of dilute wastewater constituents within the plume. On the day of the survey, the effluent temperature measured onshore prior to discharge was 9°C warmer than that of the receiving seawater at the shallow tow depth, and therefore, the presence of dilute effluent alone could not have caused the large negative thermal anomaly seen in Figure 10a. Instead, vertical temperature profiles that encountered the plume (red lines in Figure 8def) demonstrate that the 11.4°C temperature observed at the shallow tow depth matched that of the cold ambient seawater near the seafloor (red lines in Figure 8abc). Entrainment of this cold seawater shortly after discharge and its subsequent upward transport by the buoyant plume is the only mechanism that would have created the 0.7 °C temperature decrease seen in Figure 10a.

Similarly, the 2% increase in transmissivity seen within the plume during the shallow tow (shaded area south and west of the ZID in Figure 10d) could not have been created by the presence of effluent particulates within the discharge plume. Although treated effluent discharged on the day of the survey contained only a light particulate load (25.6 mg/L), its turbidity was greater than that of the receiving seawater. However, as will be demonstrated later in this report, these effluent particulates disperse rapidly shortly after discharge, and thus contribute little to the turbidity of the rising effluent plume.

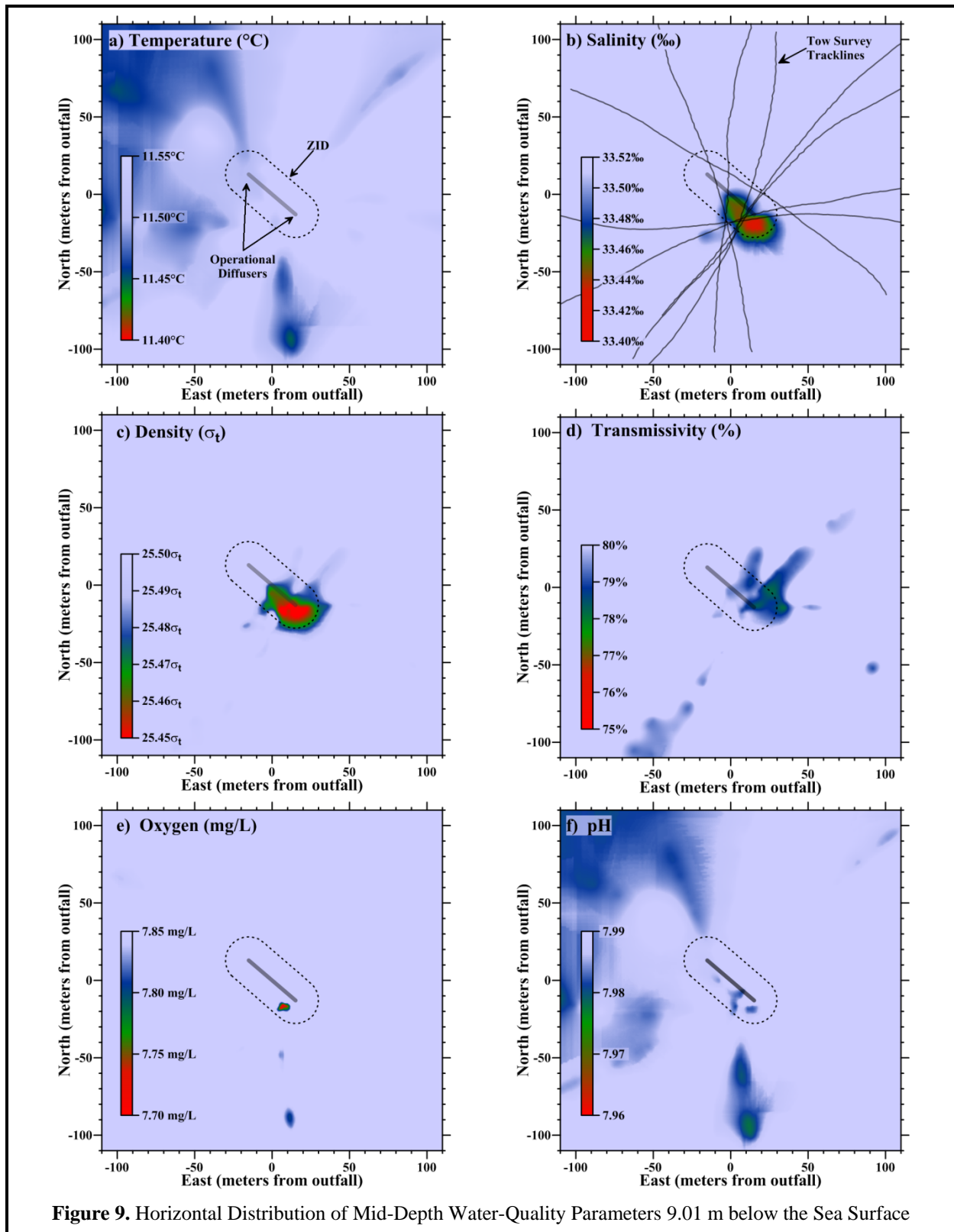


Figure 9. Horizontal Distribution of Mid-Depth Water-Quality Parameters 9.01 m below the Sea Surface

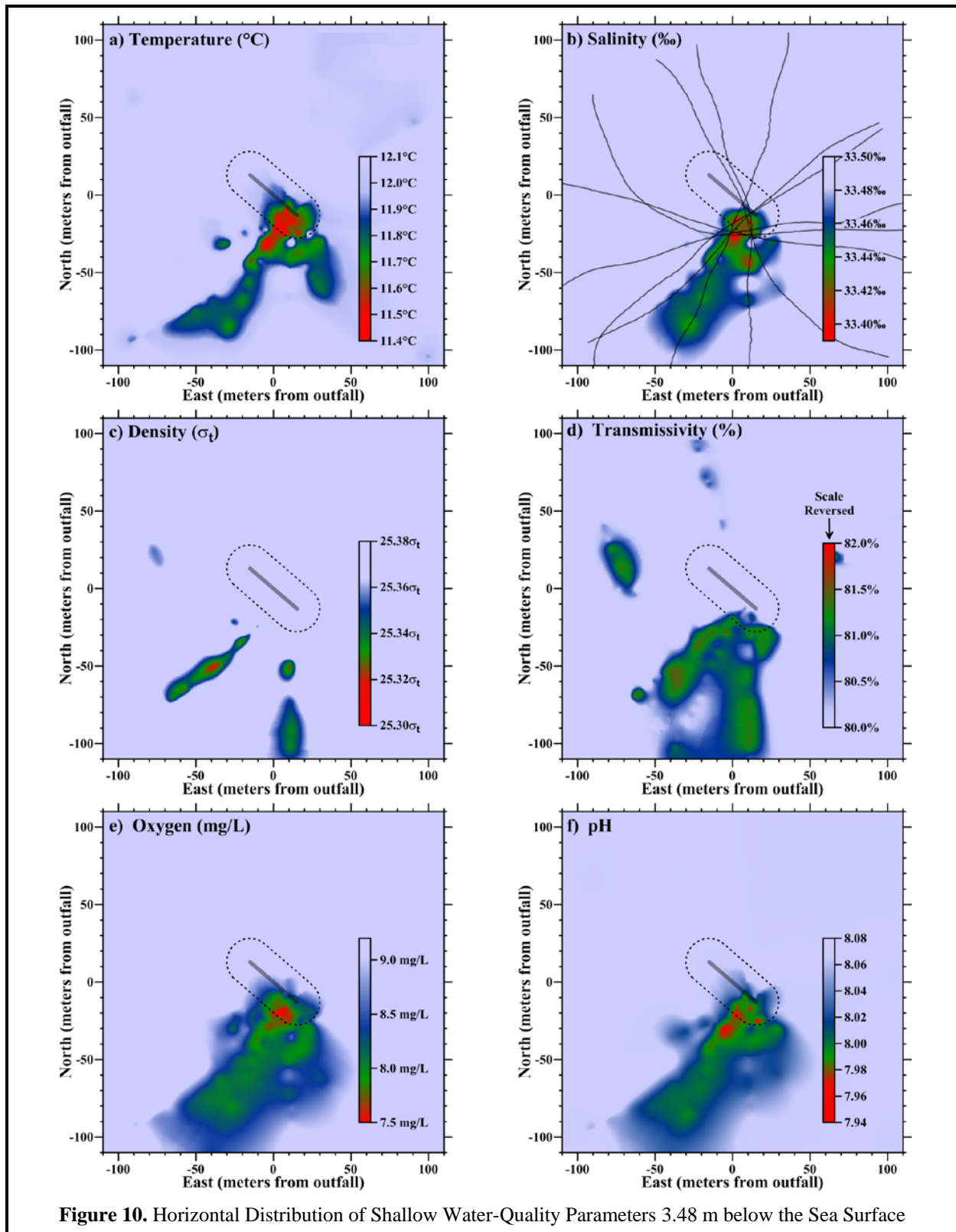


Figure 10. Horizontal Distribution of Shallow Water-Quality Parameters 3.48 m below the Sea Surface

Instead, transmissivity within the plume is largely dictated by the properties of ambient seawater entrained near the seafloor, which had higher transmissivity (85% in the light blue lines of Figure 8) than that of euphotic zone within the upper water column. Within the euphotic zone, the presence of an upwelling-induced plankton bloom naturally decreased transmissivity relative to the rest of the water column (light blue lines between 3 m and 7 m in Figure 8abc). Within this zone, the juxtaposition of the less-turbid bottom seawater entrained within the plume created the region of increased turbidity seen in Figure 10d.

It is important to distinguish plume signatures that are caused by the presence of effluent constituents, exemplified by sharp reductions in salinity and density, from those caused by the upward transport of ambient seawater entrained near the seafloor shortly after discharge, embodied by the lateral anomalies in all the other seawater properties. Close to the seafloor, intense mixing is driven by the momentum of the effluent's ejection from the individual diffuser ports. Subsequent turbulent mixing caused by the plume's ascent through the water column is less intense, and as a result, the dilute effluent plume tends to retain the ambient seawater properties it acquired at the seafloor. These deep seawater properties can become apparent as a signature of the buoyant effluent plume when they are juxtaposed against the ambient seawater characteristics in the mid and upper water column. These entrainment-generated anomalies are only apparent, however, when the water column is sufficiently stratified to cause a perceptible contrast between the shallow and deep ambient seawater properties.

The legacies of entrainment anomalies can be particularly long-lived, remaining apparent within the water column well after completion of the initial dilution process. As such, these anomalies provide useful tracers of the diffuse effluent plume during and after the completion of the initial dilution process. However, such anomalies are irrelevant to the receiving-water compliance assessment because the permit restricts attention to water-quality changes caused solely by the presence of wastewater constituents rather than by a simple relocation of ambient seawater.

At the time of the May 2016 survey, only the upper half of the water column exhibited strong stratification. Because the difference between ambient seawater properties near the seafloor and at 9 m was small, lateral anomalies in temperature, transmissivity, DO and pH (Figure 9adef) were not readily apparent at the location of the effluent plume (delineated in Figure 9bc). Entrainment anomalies only became apparent after the plume moved into the upper water column where the shallow tow took place (Figure 10adef).

Because of their longevity and greater contrast with surrounding seawater, perceptible entrainment anomalies were readily apparent over a relatively wide area in the shallow-tow maps (green and blue shading in Figure 10adef). This was the case even though effluent itself had been diluted more than 450-fold, as reflected by the 0.07‰ salinity reduction in the green and blue shaded region of Figure 10b. As described previously, the absence of a concomitant density anomaly (Figure 10c) indicates that the plume had achieved neutral buoyancy as it approached the sea surface and spread laterally. This change in plume dynamics marked the end of the initial dilution process, which is largely controlled by the effectiveness of the outfall's design.

### *Outfall Performance*

The efficacy of the outfall can be evaluated through a comparison of dilution levels measured at the time of the May 2016 survey, and dilutions anticipated from modeling studies that were codified in the discharge permit through limits imposed on effluent constituents. Specifically, the critical initial dilution

applicable to the MBCSD outfall was conservatively estimated to be 133:1 (Tetra Tech 1992). That is, dispersion modeling estimated that, at the conclusion of the minimum expected initial mixing, 133 parts of ambient seawater would have mixed with each part of wastewater.

The 133:1 dilution estimate was based on worst-case modeling under highly stratified conditions, where trapping of the plume below a strong thermocline would curtail the additional buoyant mixing normally experienced during the plume's ascent through the entire water column. Additionally, the modeling assumed quiescent oceanic flow conditions, thereby restricting initial mixing processes to the ZID. Under those conditions, the modeling predicted that a 133:1 dilution would be achieved after the plume rose only 9 m from the seafloor, whereupon it would become trapped, ceasing to ascend further in the water column. At that point, the plume would spread laterally with dilution occurring at a much-reduced rate. A 9-m ascent at the MBCSD outfall translates into a trapping depth that is 6.4 m below the sea surface. As described below, however, the dilution levels observed during the May 2016 survey were much higher than the 133:1 predicted by the modeling, and were measured at depths greater than the trapping depth predicted by the modeling.

The conservative nature of the critical initial dilution determined from the modeling is an important consideration because it was used to specify permit limitations on chemical concentrations in wastewater discharged from the treatment plant. These end-of-pipe effluent limitations were back calculated from the receiving-water objectives in the COP (SWRCB 2005) using the projected 133-fold dilution determined from the modeling. Application of a higher critical dilution would relax the stringent end-of-pipe effluent limitations thought necessary to meet COP objectives after initial dilution is complete.

End-of-pipe limitations on contaminant concentrations within discharged wastewater were based on the definition of dilution (Fischer et al. 1979). From the mass-balance of a conservative tracer, the concentration of a particular chemical constituent within effluent before discharge ( $C_e$ ) can be determined from Equation 1.

$$C_e \equiv C_o + D(C_o - C_s) \quad \text{Equation 1}$$

where:  $C_e$  = the concentration of a constituent in the effluent,  
 $C_o$  = the concentration of the constituent in the ocean after dilution by  $D$  (i.e., the COP receiving-water objective),  
 $D$  = the dilution expressed as the volumetric ratio of seawater mixed with effluent, and  
 $C_s$  = the background concentration of the constituent in ambient seawater.

By rearranging Equation 1, the actual dilution achieved by the outfall can be determined from measured seawater anomalies. This measured dilution can then be compared with the critical dilution factor determined from modeling. Salinity is an especially useful tracer because it directly reflects the magnitude of ongoing dilution. The regions of slightly lower salinity apparent south of the diffuser structure in both of the tow-survey maps (Figures 9b and 10b) were induced by the presence of dilute wastewater. These salinity anomalies document mixing processes within the effluent plume shortly after discharge, and as it subsequently rose through the water column and approached the sea surface.

The amplitudes of these salinity anomalies quantify the magnitude of wastewater dilution at the various stages of the initial mixing process. By rearranging Equation 1, the dilution ratio ( $D$ ) can be computed from the salinity anomaly ( $A = C_o - C_s$ ) as:

$$D \equiv \frac{(C_e - C_o)}{(C_o - C_s)} \propto A^{-1} \quad \text{Equation 2}$$

The salinity concentration within MBCSD effluent ( $C_e$ )<sup>18</sup> is small compared to that of the receiving seawater and, after dilution by more than 133-fold, the salinity of the effluent-seawater mixture is close to ambient salinity. Consequently, to a close approximation, dilution levels are inversely proportional to the amplitude of the salinity anomaly. Thus, a lower effluent dilution at a given location within the receiving waters is directly mirrored by a larger reduction in the measured salinity.

Among the 11,464 CTD measurements collected during the May 2016 survey, the greatest salinity reduction (-0.122‰) was recorded during the seventh transect of the mid-depth tow survey when a salinity of 33.411‰ was measured 3.3 m from the southeastern end of the diffuser structure (red shading in Figure 9b). A lower salinity (33.386‰) was measured 5.5 m southwest of the ZID boundary during the seventh transect of the shallow tow (Figure 10b) but, because the ambient salinity was also lower at that depth level (green lines at a depth of 3.5 m in Figure 8abc), the associated lateral salinity anomaly was smaller in amplitude (-0.114‰).

From Equation 2, the mid-depth salinity anomaly corresponds to a dilution of 266-fold (Figure 11), while the shallow anomaly was generated by effluent diluted 284 times (Figure 12). Both are well above the 133:1 critical initial dilution used to establish limits on contaminant concentrations in wastewater. In addition, the lowest dilution was measured at a depth of 8.6 m,<sup>19</sup> which was 2.2 m deeper than the 6.4-m trapping depth identified in the modeling that established the 133:1 minimum dilution ratio. According to the conservative modeling results, dilution levels would be expected to be substantially less than 133:1 at that depth level. Instead, the higher dilutions measured during the mid-depth tow indicate that the diffuser structure was dispersing the effluent far more efficiently than predicted by the modeling, even shortly after discharge and well before the completion of the initial dilution process.

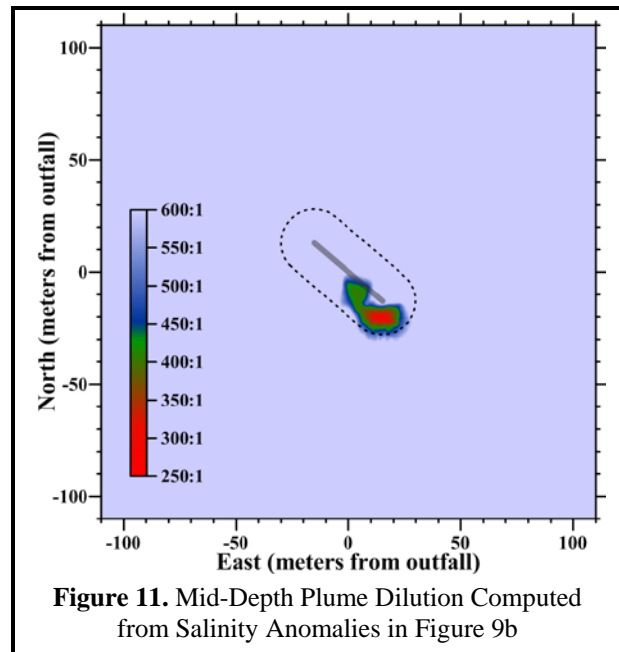


Figure 11. Mid-Depth Plume Dilution Computed from Salinity Anomalies in Figure 9b

<sup>18</sup> Wastewater samples have an average salinity of 0.995‰.

<sup>19</sup> During this portion of the seventh mid-depth transect, the CTD was tracking at a slightly shallower depth than the average 9 m reported for the entire tow.

As the buoyant plume ascended farther through the water column, it spread laterally as turbulent mixing continued to dilute the wastewater and the prevailing current transported it toward southwest (Figure 12). The lowest salinity collected during the shallow tow demonstrated that the wastewater had been diluted by at least 284-fold by the time the dilute wastewater rose an additional 5.5 m to a depth level of 3.1 m.

Overall, the dilution computations show that, during the May 2016 survey, the outfall was performing better than designed and was rapidly diluting effluent more than 266-fold almost immediately after discharge, and well before completion of the initial-dilution process. As the initial dilution process was nearing completion, effluent dilution had increased to at least 284-fold, easily exceeding the 133:1 critical initial dilution used to establish end-of-pipe permit limitations on contaminant concentrations within wastewater discharged from the MBCSD treatment plant. This demonstrates that, during the May 2016 survey, the COP receiving-water objectives were being met by the limits on chemical concentrations within discharged wastewater that are promulgated by the NPDES discharge permit issued to the MBCSD.

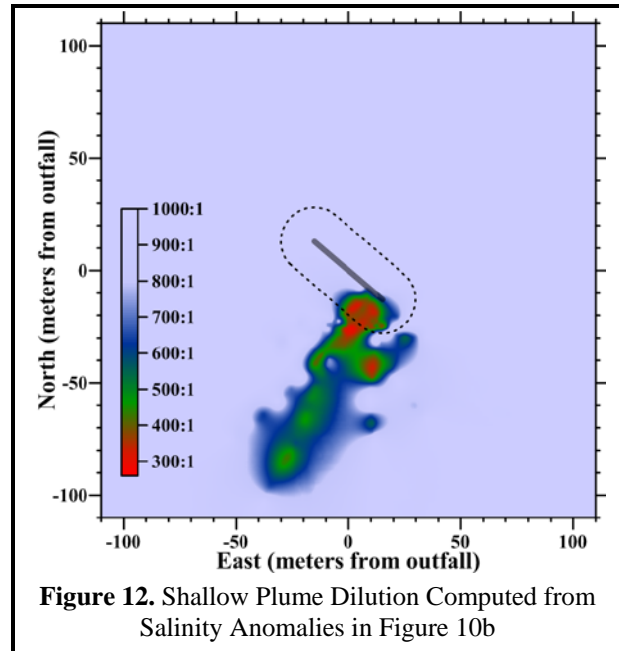


Figure 12. Shallow Plume Dilution Computed from Salinity Anomalies in Figure 10b

### COMPLIANCE

This section evaluates compliance with the water-quality limitations listed in the NPDES permit (Table 6). The limits themselves are based on criteria in the COP, the Central Coast Basin Plan, and other state and federal policies that were designed to protect marine life and beneficial uses of ocean waters. Because the limits only pertain to changes in water properties that are caused by the presence of wastewater constituents beyond the ZID, instrumental measurements undergo a series of screening procedures prior to numeric comparison with the permit thresholds. Specifically, the quantitative analyses described in this section focus on water-property excursions caused by the presence of wastewater constituents beyond the ZID, whose amplitudes can be reliably discerned against the backdrop of ambient fluctuations. A detailed understanding of ambient seawater properties, and their natural variability within the region surrounding the outfall, is therefore an integral part of the compliance evaluation presented in this section.

Table 6. Permit Provisions Addressed by the Offshore Receiving-Water Surveys

Limit #	Limit
P1	Floating particles or oil and grease to be visible on the ocean surface
P2	Aesthetically undesirable discoloration of the ocean surface
P3	Temperature of the receiving water to adversely affect beneficial uses
P4	Significant reduction in the transmittance of natural light at any point outside the ZID
P5	The DO concentration outside the zone of initial dilution to fall below 5.0 mg/L or to be depressed more than 10% from that which occurs naturally
P6	The pH outside the zone of initial dilution to be depressed below 7.0, raised above 8.3, or changed more than 0.2 units from that which occurs naturally

The results of these analyses of the May 2016 data demonstrate that the MBCSD discharge complied with the NPDES discharge permit. Moreover, although observations within the ZID are not subject to compliance evaluations, they met the prescribed limits because actual dilution levels routinely exceeded the conservative design specifications assumed in the discharge permit. Thus, the quantitative evaluation described in this section documents an outfall and treatment process that was performing at a high level during the May 2016 survey.

### *Permit Provisions*

The offshore receiving-water surveys are designed to assess compliance with objectives dealing with undesirable alterations to six physical and chemical characteristics of seawater. Specifically, the permit states that wastewater constituents within the discharge shall not cause the limits listed in Table 6 to be exceeded.

The first two receiving-water limits, P1 and P2, rely on qualitative visual observations for compliance evaluation. Compliance was demonstrated during the May 2016 survey through visual inspection of the sea surface that found an absence of floating wastewater materials, oil, grease, and discoloration of the sea surface.

Compliance with the remaining four receiving-water limitations is quantitatively evaluated through a comparison between instrumental measurements and numerical limits listed in the NPDES permit. For example, in P5 and P6, the fixed numeric limits on absolute values of DO (>5 mg/L) and pH (7.0 to 8.3) can be directly compared with field measurements within the dilute wastewater plume beyond the ZID. However, both P5 and P6 also contain narrative limits, which originate in the COP, and define unacceptable water-quality impacts in terms of “*significant*” excursions beyond those that occur “*naturally*.” Quantitative evaluation of these limits requires a further comparison of field measurements with numerical thresholds that reflect the natural variation in transmissivity, DO, and pH within the receiving waters surrounding the outfall.

As described previously, natural variation in seawater properties can result from a variety of oceanographic processes. These processes establish the range in ambient seawater properties caused by natural spatial variation within the survey region at a given time (e.g., vertical stratification), and by temporal variations caused by seasonal and interannual influences (e.g., El Niño and La Niña). Of particular interest are upwelling and downwelling processes that not only determine average properties at a given time, but also the degree of water-column stratification, or spatial variability, present during any given survey.

### *Screening of Measurements*

Evaluating whether any of the 11,464 CTD measurements collected during the May 2016 survey exceeded a permit limit can be a complex process. For example, although apparently significant excursions in an individual seawater property may be related to the presence of wastewater constituents, they may also result from instrumental errors, natural processes, entrainment of ambient bottom waters in the rising effluent plume, statistical uncertainty, ongoing initial mixing within and beyond the ZID, or other anthropogenic influences (e.g., dredging discharges or oil spills).

Because of this complexity, measurements were first screened to determine whether numerical limits on individual seawater properties apply (Table 7). The screening procedure sequentially applies three questions to restrict attention to: 1) the oceanic area where permit provisions pertain; 2) changes due to the presence of wastewater particulates; and 3) changes large enough to be reliably detected against the backdrop of natural variation. The measurements that remain after completing the screening process can then be compared with Basin-Plan numerical limits and COP allowances.

**Table 7. Receiving-Water Measurements Screened for Compliance Evaluation**

Topic Addressed	Screening Question	Answer		Parameter
		No	Yes <sup>20</sup>	
Location	1. Was the measurement collected beyond the 15.2-m ZID boundary where modeling assumes that initial dilution is complete?	1,521	9,943	All
Wastewater Constituents	2. Did the beyond-ZID measurement coincide with a quantifiable salinity anomaly ( $\leq 550:1$ dilution level) indicating the presence of detectable wastewater constituents?	9,682	261	All
Natural Variation	3. Did seawater properties associated with the wastewater measurements depart significantly from the expected range in ambient seawater properties at the time of the survey?	261	0	Temperature
		261	0	Transmissivity
		261	0	DO
		261	0	pH

The following subsection provides additional lines-of-evidence that demonstrate compliance with numerical permit limits independent of the screening process. The rationale for identifying observations suitable for further compliance analysis is presented in the following descriptions of the three screening steps.

**1. Measurement Location:** The COP states that compliance with its receiving-water objectives “shall be determined from samples collected at stations representative of the area within the waste field where initial dilution is completed.” Initial dilution includes the mixing that occurs from the turbulence associated with both the ejection jet, and the buoyant plume’s subsequent ascent through the water column.

Although currents often transport the plume well beyond the ZID before the initial dilution process is complete, the COP states that dilution estimates shall be based on “the assumption that no currents, of sufficient strength to influence the initial dilution process, flow across the discharge structure.” Because of this, the regulatory mixing distance, which is equal to the 15.2-m water depth of the discharge, provides a conservative boundary to screen receiving-water data for subsequent compliance evaluation. Application of this initial screening question to the May 2016 dataset eliminated 1,521 of the original 11,464 receiving-water observations from further consideration because they were collected within the ZID (Table 7, Question 1). The remaining 9,943 observations were carried forward in the screening analysis.

**2. Presence of Wastewater Constituents:** The MBCSD discharge permit restricts application of the numerical receiving-water limits to excursions caused by the presence of wastewater constituents. This confines the compliance analysis to changes caused “as the result of the discharge of waste,” as specified in the COP, rather than anomalies that arise from the upward movement of ambient seawater entrained

<sup>20</sup> Number of remaining CTD observations of potential compliance interest based on sequential application of each successive screening question

within the buoyant effluent plume. Analyses conducted on quarterly receiving-water surveys over the last decade have demonstrated that the direct influence of dilute wastewater is almost never observed in any seawater property other than salinity, except very close (<1 m) to a diffuser port and within its ejection jet.

In fact, negative salinity anomalies are the only consistent indicator of the presence of wastewater constituents within receiving waters. Wastewater salinity is negligible compared to that of the receiving seawater, so the presence of a distinct salinity minimum provides *de facto* evidence of the presence of wastewater constituents. Because of the large contrast between the nearly fresh wastewater and the salty receiving water, salinity provides a powerful tracer of dilute wastewater that is unrivaled by other seawater properties. Other properties do not exhibit such a large contrast and, as such, their wastewater signatures dissipate rapidly upon discharge with very little mixing. Wastewater's lack of salinity, however, provides a definitive tracer that allows the presence of effluent constituents to be identified even after dilution many times greater than the 133-fold critical initial dilution assumed in the discharge permit.

As described in the previous section, wastewater-induced reductions in salinity can be used to determine the amount of dilution achieved by initial mixing. Based on statistical analyses of the natural variability in salinity readings measured near the outfall over a five-year period between 2004 and 2008, the smallest reduction in salinity that can be reliably detected within receiving waters is 0.062‰. This represents a dilution level of 542-fold in Equation 2. Salinity reductions that are smaller than 0.062‰ cannot be reliably discerned against the backdrop of natural variation, and would not result in discernible changes in other seawater properties. Eliminating those measurements from further evaluation restricts attention to excursions in temperature, light transmittance, DO, and pH that are potentially related to the presence of wastewater constituents.

As discussed previously, the greatest salinity reduction observed during the May survey was recorded very close to the diffuser structure during the mid-depth tow survey. Somewhat smaller salinity reductions associated with more dilute portions of the plume were measured beyond the southern boundary of the ZID during vertical profiling at Station RW4, and during the shallow tow. A total of 261 of the salinity reductions measured beyond the ZID corresponded to dilutions less than 550:1 (Table 7). The remaining 9,682 observations that were measured outside the ZID during the May 2016 survey did not have salinity reductions that were greater than the 0.062‰ plume-detection threshold.

**3. Natural Variation:** An integral part of the compliance analysis is determining whether a particular anomalous measurement resulted from the presence of wastewater constituents, or whether it simply became apparent because ambient seawater was relocated (upward) by the plume. If the measurement does not significantly depart from the natural range in ambient seawater properties at the time of the survey, then it is difficult to ascribe the departure to the presence of wastewater constituents. Thus, quantifying the natural variability around the outfall at the time of the survey is necessary for determining whether a particular observation warrants comparison with the numeric permit limits.

A statistical analysis of receiving-water data collected around the outfall was used to establish the range in natural conditions surrounding the outfall (first three data columns of Table 8). These ambient-variability ranges were used to identify significant departures from natural conditions that could be indicative of adverse discharge-related effects on water quality. The same five-year database used to establish the within-survey salinity variation discussed previously, was also used to establish one-sided 95% confidence bounds on transmissivity (-10.2%), temperature (+0.82°C), DO (-1.38 mg/L), and pH ( $\pm 0.094$ ). These were combined with 95<sup>th</sup> percentiles determined from the May 2016 ambient seawater data, to establish time-specific natural-variability thresholds in a manner analogous to COP Appendix VI. The

percentiles were largely determined from May 2016 vertical profile data collected at northern Stations RW1, RW2, and RW3, thereby excluding measurements potentially affected by the discharge.

**Table 8. Compliance Thresholds**

Water Quality Property	95% Confidence Bound <sup>21</sup>	95 <sup>th</sup> Percentile <sup>22,23</sup>	Natural Variability Threshold <sup>24</sup>	COP Allowance <sup>25</sup>	Basin Plan Limit <sup>26</sup>	Extremum <sup>27</sup>
Temperature (°C)	0.82	12.93	>13.75	—	—	≤13.19
Transmissivity (%)	-10.2	78.9	<68.7	—	—	≥74.9
DO (mg/L)	-1.38	6.87	<5.49	<4.94	<5.00	≥6.73
pH (minimum)	-0.094	7.936	<7.842	<7.642	<7.000	≥7.922
pH (maximum)	0.094	8.099	>8.193	>8.393	>8.300	≤8.102

Temperature, transmissivity, pH, and DO concentrations associated with the 261 remaining measurements of potential compliance interest were all well within their respective ranges of natural variability (Table 7, Question 3). As such, the screening process unequivocally eliminated all of the measurements collected during the May 2016 survey from further consideration in the compliance analysis. In fact, all of the documented excursions in these properties were the result of physical processes unrelated to the presence of wastewater constituents, namely, entrainment of near-bottom seawater within the rising effluent plume.

As described previously, anomalies in seawater properties clearly delineated the plume, but those entrainment-generated excursions were not caused by the presence of wastewater constituents. During periods when the water column is even slightly stratified, ambient seawater properties near the seafloor differ from those within the rest of the water column, and their juxtaposition within the rising effluent plume appears as lateral anomalies within the upper water column. Regardless, if the presence of wastewater particulates had contributed to the observed decreases in DO and pH within the upper water column, their influence would still have been well within the natural range of the ambient seawater properties at the time of the survey. Consequently, their influence on water quality would not be considered environmentally significant.

<sup>21</sup> The one-sided confidence bound measures the ability to reliably determine ambient seawater properties within surveys as a whole. They were determined from an analysis of the variability in ambient water-quality data collected during 20 quarterly surveys conducted between 2004 and 2008. Although water-quality observations potentially affected by the presence of wastewater constituents were excluded from the analysis, more than 9,200 remaining observations for each of the six seawater properties accurately quantified the inherent uncertainty in defining the range in natural conditions.

<sup>22</sup> The COP (Appendix I, Page 27, SWRCB 2005) defines a “significant” difference as “a statistically significant difference in the means of two distributions of sampling results at the 95% confidence level.” Accordingly, COP effluent analyses (Step 9 in Appendix VI, Page 42, Ibid.) are based “the one-sided, upper 95% confidence bound for the 95th percentile.”

<sup>23</sup> The 95<sup>th</sup>-percentile quantified natural variability in seawater properties during the May 2016 survey itself, and was determined from vertical-profiles data unaffected by the discharge.

<sup>24</sup> Thresholds represent limits on wastewater-induced changes to receiving-water properties that significantly exceed natural conditions as specified in the discharge permit and COP. They are determined from the sum of columns to the left and are specific to the May 2016 survey. They do not include the COP allowances specified in the column to the right.

<sup>25</sup> The discharge permit, in accordance with the COP, allows excursions in seawater properties that depart from natural conditions by specified amounts. DO cannot be “depressed more than 10% from that which occurs naturally,” and pH cannot be “changed more than 0.2 units from that which occurs naturally.”

<sup>26</sup> Permit limits P5 and P6 (Table 6) include specific numerical values promulgated in the RWQCB Basin Plan (1994) in addition to changes relative to natural conditions specified in the COP. The Basin Plan upper-bound pH objective for ocean waters is 8.5, but a more-stringent upper-bound objective of 8.3, which applies to individual beneficial uses, was implemented in the MBCSD discharge permit.

<sup>27</sup> Maximum or minimum value measured during the May 2016 survey, regardless of location within or beyond the ZID

### *Other Lines of Evidence*

Several additional lines of evidence further support the conclusion that all the CTD measurements collected during the May 2016 survey complied with permit limits P3 through P6 in Table 6. In combination, these lines of evidence provide the “best explanation” of the origin and significance of individual measurements using abductive inference (Suter 2007). This process, which has been used to implement sediment-quality guidelines for California estuaries (SWRCB 2009), emphasizes a pattern of reasoning that accounts for both discrepancies and concurrences among multiple lines of evidence. A best explanation approach serves to limit the uncertainty associated with each individual CTD measurement, and to provide a more robust compliance assessment. Together, these lines of evidence significantly strengthen the conclusion that the discharge fully complied with the permit at the time of the May 2016 survey.

***Insignificant Thermal Impact:*** Although there are no explicit numerical objectives for discharge-related increases in temperature, a numerical limit can be established for thermal excursions that is based on the requirement that they not adversely affect beneficial uses (P3 in Table 6). Increases in temperature caused by the discharge of warm wastewater could be deemed to affect beneficial uses adversely if they exceeded the natural temperature range observed at the time of the survey (i.e. exceeded 13.75°C listed in the third data column of Table 8). However, none of the 11,464 CTD measurements collected during the May 2016 survey exceeded 13.19°C (last column in Table 8). Additionally, as mentioned previously, because the effluent entrained cooler bottom water shortly after discharge, the rising plume actually exhibited a lower temperature than the surrounding seawater in the upper water column (Figure 10a).

***Limited Ambient Light Penetration:*** As with temperature, there are no explicit numerical objectives for discharge-related decreases in transmissivity. However, the COP narrative objective (P4) limiting significant reductions in the transmission of natural light can also be translated into a numerical objective. Specifically, because the COP does not specify an allowance beyond natural conditions, the same 68.7% threshold on ambient transmissivity variations listed in third data column of Table 8 can be interpreted to constitute a numerical limit.

However, none of the transmissivity measurements collected during the May 2016 survey fell below the 68.7% minimum compliance threshold. The lowest transmissivities measured during the survey (74.9%) were recorded at a depth of 3.8 m and at a location well beyond the influence of the discharge. As described previously, increased turbidity (reduced transmissivity) between 3 m and 7 m within the upper water column was a natural consequence of upwelling, namely, enhancement of primary production by the upward transport of nutrients into the euphotic zone.

Moreover, the COP objective for light penetration only applies to a small portion of the transmissivity measurements. Because little natural light is present beneath the euphotic zone, which extends to approximately twice the Secchi depth, the limit on transmissivity reductions during the May 2016 survey only applies to measurements recorded above 8.5 m (twice the average Secchi depth listed in Table 4). Consequently, even if the discharge of wastewater particulates had caused one or more of the 4,229 transmissivity measurements collected below the euphotic zone to drop below the numeric compliance threshold, it would not have been of regulatory concern because the penetration of ambient light would not have been affected.

***Directional Offset:*** Analysis of the directional offset of CTD measurements is useful because wastewater and receiving-seawater properties depart from one another in several predictable ways. Specifically, upon discharge, wastewater is fresher, warmer, and lighter than the ambient receiving waters of Estero Bay. Under most conditions, wastewater is also more turbid than the receiving waters because of organic particulates suspended in the treated effluent. As such, the presence of wastewater constituents will reduce the salinity, density, and transmissivity of the receiving seawater (negative offset), while

temperature will be increased (positive offset). Therefore, as discussed previously, the reduced temperatures observed in conjunction with the effluent plume in the upper water column (Figure 10a) could not have been generated by the presence of warmer wastewater constituents. Similarly, the increased transmissivity observed within the discharge plume during the shallow tow (Figure 10d) could not have been generated by an unacceptably high particulate load within wastewater. In both cases, the directional offsets were opposite of receiving-water impacts expected from the presence of wastewater constituents.

***Insignificant Wastewater Particulate Loads:*** Another independent line of evidence demonstrates that the discharge of wastewater particulates could not have contributed materially to turbidity within the dilute effluent plume. The suspended-solids concentration measured onshore, within the effluent, and immediately prior to discharge from the WWTP on 24 May 2016 was 25.6 mg/L. After dilution by at least 266-fold, the effluent suspended-solids concentration would have the reduced ambient transmissivity by no more than 0.7%. This small potential decrease in transmissivity is overwhelmed by the large 5.2% decrease in ambient transmissivity caused by the increased presence of plankton within the thermocline during upwelling.

Similarly, the MBCSD discharge could not have contributed materially to the observed DO fluctuations. The MBCSD treatment process routinely removes 80% or more of the organic material, as demonstrated by the low, 49-mg/L BOD measured within the plant's effluent two days after the survey. That small amount of BOD would have induced a DO depression of no more than 0.022 mg/L after dilution (MRS 2002). In fact, in the absence of tangible BOD influence, wastewater discharge would actually be expected to increase DO within subsurface receiving waters, rather than decrease it. This is because effluent is oxygenated by recent contact with the atmosphere during the treatment process, whereas receiving waters at depth are typically depleted in DO due to the lack of atmospheric equilibration within the deep offshore watermass.

***COP Allowances:*** The COP does not explicitly require that wastewater-induced changes remain within the ranges in natural variation listed in the third data column of Table 8, even though these ranges were conservatively used in the data screening process described in previous subsections. Consideration of these COP allowances for receiving-water limits provides an additional safety factor in the compliance evaluation.

For pH, the COP and the discharge permit allow changes up to 0.2 pH units from natural conditions, bringing the minimum allowed pH down to 7.642 during the May 2016 survey (fourth data column of Table 8). This limiting value is significantly less than the lowest pH measurement of 7.922 recorded during the May 2016 survey (last column of Table 8).<sup>28</sup> Similarly, the lowest DO concentration measured during the survey (6.73 mg/L) was well above both the lower range in natural variation (5.49 mg/L) and the 10% compliance threshold promulgated by the COP (4.94 mg/L).

***Excursions remained within the fixed Basin-Plan Limits:*** Permit provisions P5 and P6 (Table 6) combine receiving-water objectives from both the COP and the Basin Plan with regard to DO and pH limitations. As described previously, the COP requires that DO concentrations outside the ZID not be depressed more than 10% from that which occurs naturally, and restricts pH measurements to those within 0.2 units of that which occurs naturally. In contrast, the Basin-Plan's fixed numerical limits do not provide specific guidance as to how they might change in response to widespread changes in oceanographic conditions unrelated to the discharge. Specifically, the fixed numerical limits restrict DO concentrations outside the ZID to no less than 5 mg/L (P5 in Table 6), and pH levels to the 7.0-to-8.3

<sup>28</sup> Compliance with COP maximum pH allowance (8.393) is irrelevant because effluent on the day of the survey had a pH of 7.6, which is much lower than the lowest pH measured within the receiving seawater (7.922). Consequently, the presence of effluent constituents could not have induced an increase in pH within receiving waters.

range (P6). As such, the fixed Basin-Plan limit on DO is slightly more restrictive than the 4.94 mg/L minimum allowable DO concentration established for the May 2016 survey under COP objectives; yet the all of the DO measurements also complied with the more conservative Basin-Plan limit on DO reductions. Similarly, the maximum allowable pH (8.3) specified in the Basin Plan was more restrictive than the COP limit (8.393) specified for the May 2016 Survey, yet all the measurements again complied with both regulations.

**Natural Variability within and beyond the ZID:** Although the permit limits only apply to changes in DO, pH, temperature, and transmissivity beyond the ZID, examination of measurements acquired within the ZID frequently provides additional insight into the potential for adverse effects on water quality. However, among all the data collected during the May 2016 survey, salinity was the only seawater property that exhibited a perceptible difference from ambient conditions. Regardless of their association with the plume's effluent salinity signature or their proximity to the diffuser structure, none of the 11,464 temperature, DO, pH, and transmissivity observations exceeded the thresholds of natural variability specified in Table 8.

## CONCLUSIONS

The quantitative screening analysis demonstrated that all measurements recorded during the May 2016 survey complied with the receiving-water limitations specified in the NPDES discharge permit. This conclusion was further strengthened by other lines of evidence supporting compliance with the discharge permit. Specifically, although discharge-related changes in seawater properties were observed during the May 2016 survey, the changes were either not of significant magnitude (i.e., they were within the natural range of variability that prevailed at the time of the survey), were measured within the boundary of the ZID where initial mixing is still expected to occur, or were not directly caused by the presence of wastewater constituents within the water column (i.e., were entrainment generated).

Shortly after discharge, and well before the initial dilution process was complete, the effluent was achieving dilution levels in excess of 266-fold, which is well more than the critical dilution levels predicted by design modeling. As the plume ascended through the water column and approached the sea surface near the completion of the initial mixing process, dilution levels exceeded 284-fold. All of the measured dilution levels far exceeded levels that were predicted by modeling and that were incorporated in the discharge permit as limits on contaminant concentrations within effluent prior to discharge. Lastly, all of the auxiliary observations collected during the May 2016 survey demonstrated that the discharge complied with the narrative receiving-water limits in the discharge permit and the COP. Together; these observations demonstrate that the treatment process, diffuser structure, and the outfall continue to surpass design expectations.

## REFERENCES

- Davis, R.E., J.E. Dufour, G.J. Parks, and M.R. Perkins. 1982. Two Inexpensive Current-Following Drifters. Scripps Institution of Oceanography, University of California, San Diego, La Jolla, California. SIO Reference No. 82-28. December 1982.
- Fischer, H.B., E.J. List, R.C.Y. Koh, J. Imberger, and N.H. Brooks. 1979. Mixing in Inland and Coastal Waters. New York: Academic Press, 482 p.
- Kuehl, S.A., C.A. Nittrouer, M.A. Allison, L. Ercilio, C. Faria, D.A. Dukat, J.M. Jaeger, T.D. Pacioni, A.G. Figueiredo, and E.C. Underkoffler 1996. Sediment deposition, accumulation, and seabed dynamics in an energetic fine-grained coastal environment. *Continental Shelf Research*, 16: 787-816.

- Marine Research Specialists (MRS). 1998. City of Morro Bay and Cayucos Sanitary District, Offshore Monitoring and Reporting Program, Semiannual Benthic Sampling Report, April 1998 Survey. Prepared for the City of Morro Bay, CA. July 1998.
- Marine Research Specialists (MRS). 2002. City of Morro Bay and Cayucos Sanitary District, Supplement to the 2002 Renewal Application For Ocean Discharge Under NPDES Permit No. Prepared for the City of Morro Bay and Cayucos Sanitary District, Morro Bay, CA. July 2002.
- [Marine Research Specialists \(MRS\). 2011. City of Morro Bay and Cayucos Sanitary District, Offshore Monitoring and Reporting Program, 2010 Annual Report. Prepared for the City of Morro Bay, California. March 2011.](#)
- [Marine Research Specialists \(MRS\). 2012. City of Morro Bay and Cayucos Sanitary District, Offshore Monitoring and Reporting Program, 2011 Annual Report. Prepared for the City of Morro Bay, California. March 2012.](#)
- [Marine Research Specialists \(MRS\). 2013. City of Morro Bay and Cayucos Sanitary District, Offshore Monitoring and Reporting Program, 2012 Annual Report. Prepared for the City of Morro Bay, California. March 2013.](#)
- Marine Research Specialists (MRS). 2014. City of Morro Bay and Cayucos Sanitary District, Offshore Monitoring and Reporting Program, 2013 Annual Report. Prepared for the City of Morro Bay, California. March 2014.
- National Academy of Sciences. 1993. Managing Wastewater in Coastal Urban Areas. National Research Council Committee on Wastewater Management for Coastal Urban Areas, Water Science and Technology Board, Commission on Engineering and Technical Systems. 477 pp.
- Regional Water Quality Control Board (RWQCB) - Central Coast Region. 1994. Water Quality Control Plan (Basin Plan) Central Coast Region. Available from the RWQCB at 81 Higuera Street, Suite 200, San Luis Obispo, California. 148p. + Appendices.
- Regional Water Quality Control Board (RWQCB) - Central Coast Region and the Environmental Protection Agency (USEPA) – Region IX. 1992a. Waste Discharge Requirements (Order No. 92-67) and Authorization to Discharge under the National Pollutant Discharge Elimination System (Permit No. CA0047881) for City of Morro Bay and Cayucos Sanitary District, San Luis Obispo County.
- Regional Water Quality Control Board (RWQCB) - Central Coast Region and the Environmental Protection Agency (USEPA) – Region IX. 1992b. Monitoring and Reporting Program No. 92-67 for City of Morro Bay and Cayucos Sanitary District, San Luis Obispo County (Permit No. CA0047881).
- Regional Water Quality Control Board (RWQCB) - Central Coast Region and the Environmental Protection Agency (USEPA) – Region IX. 1998a. Waste Discharge Requirements (Order No. 98-15) and National Pollutant Discharge Elimination System (Permit No. CA0047881) for City of Morro Bay and Cayucos Sanitary District, San Luis Obispo County. 11 December 1998.
- Regional Water Quality Control Board (RWQCB) - Central Coast Region and the Environmental Protection Agency (USEPA) – Region IX. 1998b. Monitoring and Reporting Program No. 98-15 for City of Morro Bay and Cayucos Sanitary District, San Luis Obispo County. 11 December 1998.

- Regional Water Quality Control Board (RWQCB) - Central Coast Region and the Environmental Protection Agency (EPA) – Region IX. 2009. Waste Discharge Requirements (Order No. R2-2008-0065) and National Pollutant Discharge Elimination System (Permit No. CA0047881) for the Morro Bay and Cayucos Wastewater Treatment Plant Discharges to the Pacific Ocean, Morro Bay, San Luis Obispo County. Effective 1 March 2009.
- Sea-Bird Electronics, Inc. (SBE) 1989. Calculation of M and B Coefficients for the Sea-Tech Transmissometer. Application Note No. 7, Revised September 1989.
- Sea-Bird Electronics, Inc. (SBE) 1992. SBE 12/22/22/20 Dissolved Oxygen Sensor Calibration and Deployment. Application Note No. 12-1, rev B, Revised April 1992.
- Southern California Bight Field Methods Committee (SCBFMC). 2002. Field Operation Manual for Marine Water-Column, Benthic, and Trawl monitoring in Southern California. Technical Report 259. Southern California Coastal Water Research Project. Westminster, CA. March 2002.
- State Water Resources Control Board (SWRCB). 2005. Water Quality Control Plan, Ocean Waters of California, California Ocean Plan. California Environmental Protection Agency. Effective February 14, 2006.
- State Water Resources Control Board (SWRCB). 2009. Water Quality Control Plan for Enclosed Bays and Estuaries – Part 1 Sediment Quality. California Environmental Protection Agency. Effective August 22, 2009. [sed\\_qlty\\_part1.pdf](#) [Accessed 02/26/10].
- Suter II, Glenn, W. 2007. Ecological risk assessment, 2nd edition. U. S. Environmental Protection Agency, Cincinnati, Ohio. CRC.
- Tetra Tech. 1992. Technical Review City of Morro Bay, CA Section 201(h) Application for Modification of Secondary Treatment Requirements for a Discharge into Marine Waters. Prepared for the U.S. Environmental Protection Agency, Region IX, San Francisco, CA by Tetra Tech, Inc., Lafayette, CA. February 1992.